Shedding of syndecan-4 promotes immune cell recruitment and mitigates cardiac dysfunction after lipopolysaccharide challenge in mice. Strand ME, Aronsen JM, Braathen B, Sjaastad I, Kvaløy H, Tønnessen T, Christensen G, Lunde IG. J Mol Cell Cardiol. 2015 Nov;88:133-44

Shedding of syndecan-4 promotes immune cell recruitment and mitigates cardiac dysfunction after lipopolysaccharide challenge in mice

Mari E. Strand[a,b], Jan Magnus Aronsen[c], Bjørn Braathen[d], Ivar Sjaastad[a,b], Heidi Kvaløy[a,b], Theis Tønnessen[b,d], Geir Christensen[a,b], Ida G. Lunde[a,b,e]

[a] Institute for Experimental Medical Research, Oslo University Hospital and University of Oslo, Oslo, Norway
[b] KG Jebsen Cardiac Research Center and Center for Heart Failure Research, University of Oslo, Oslo, Norway
[c] Bjørknes College, Oslo, Norway
[d] Department of Cardiothoracic Surgery, Oslo University Hospital Ullevål, Oslo, Norway
[e] Department of Genetics, Harvard Medical School, Boston, MA, USA

Corresponding author:
Mari E. Strand
Institute for Experimental Medical Research, Oslo University Hospital Ullevål,
Kirkeveien 166, Building 7, 4th floor, 0407 Oslo, Norway
Phone: +4723016800/ Fax: +4723016799
E-mail: m.e.strand@medisin.uio.no

Abstract

Inflammation is central to heart failure progression. Innate immune signaling increases expression of the transmembrane proteoglycan syndecan-4 in cardiac myocytes and fibroblasts, followed by shedding of its ectodomain. Circulating shed syndecan-4 is increased in heart failure patients, however the pathophysiological and molecular consequences associated with syndecan-4 shedding remain poorly understood. Here we used lipopolysaccharide (LPS) challenge to investigate the effects of syndecan-4 shedding in the heart.

Wild-type mice (10mg/kg, 9h) and cultured neonatal rat cardiomyocytes and fibroblasts were subjected to LPS challenge. LPS increased cardiac syndecan-4 mRNA without altering full-length protein. Elevated levels of shedding fragments in the myocardium and blood from the heart confirmed syndecan-4 shedding *in vivo*. A parallel upregulation of ADAMTS1, ADAMTS4 and MMP9 mRNA suggested these shedding enzymes to be involved. Echocardiography revealed reduced ejection fraction, diastolic tissue velocity and prolonged QRS duration in mice unable to shed syndecan-4 (syndecan-4 KO) after LPS challenge. In line with syndecan-4 shedding promoting immune cell recruitment, expression of immune cell markers (CD8, CD11a, F4/80) and adhesion receptors (Icam1, Vcam1) were attenuated in syndecan-4 KO hearts after LPS. Cardiomyocytes and fibroblasts exposed to shed heparan sulfate-substituted syndecan-4 ectodomains showed increased Icam1, Vcam1, TNFα and IL-1β expression and NF-κB-activation, suggesting direct regulation of immune cell recruitment pathways. In cardiac fibroblasts, shed ectodomains regulated expression of extracellular matrix constituents associated with collagen synthesis, cross-linking and turnover. Higher syndecan-4 levels in the coronary sinus vs. the radial artery of open heart surgery patients suggested that syndecan-4 is shed from the human heart.

Our data demonstrate that shedding of syndecan-4 ectodomains is part of the cardiac innate immune response, promoting immune cell recruitment, extracellular matrix remodeling and mitigating cardiac dysfunction in response to LPS.

Keywords: proteoglycan, fibrosis, innate immunity, sepsis, heart failure

1. Introduction

Activation of the innate immune system is central to heart failure progression, promoting cardiac inflammation, remodeling and dysfunction [1, 2]. Clinical therapies targeting inflammation are yet to show benefits for heart failure patients, reflecting a need for an improved understanding of mechanisms underlying the immune responses of the heart [3]. Proteoglycans are proteins substituted with glycosaminoglycan chains (GAGs). The four-membered syndecan family (syndecan-1-4) of transmembrane proteoglycans carry heparan sulfate (HS) GAGs on their ectodomains, binding numerous extracellular matrix (ECM) ligands, immune cells and inflammatory mediators. The syndecan family is implicated in key events of the inflammatory cascade in tissue injury and wound healing [4].

Syndecans associate with various ECM proteases [5] that cleave and release the HS-substituted ectodomain from the cell surface in a process called shedding [6]. The extracellular cleavage domain and the GAG attachment sites are highly conserved among species, indicating an important function for the shed, GAG-substituted ectodomain [7]. Shedding of syndecans from epithelial cells is accelerated during wound healing and the soluble ectodomains are believed to orchestrate aspects of the inflammatory response such as immune cell recruitment [8-10].

In the heart, syndecan-4 mRNA and protein are upregulated during heart failure progression after pressure overload and infarction in mice and patients [11-14]. Syndecan-4 is expressed in cardiac myocytes and fibroblasts, and we recently found that syndecan-4 is upregulated in both cell types by tumor necrosis factor (TNF)α, interleukin (IL)-1β and lipopolysaccharide (LPS) through a functional nuclear factor (NF)-κB site in its promoter [15]. LPS is a component of Gram-negative bacteria that through toll-like receptor 4 (TLR4) activates the innate immune system, elevating NF-κB signaling and TNFα and IL-1β levels [16]. Importantly, we showed that subsequent to its upregulation by innate immune signaling, syndecan-4 was shed from the surface of cultured cardiac myocytes and fibroblasts [15], suggesting syndecan-4 shedding to be an effector of the innate immune response. Thus, identification of pathophysiological and molecular consequences associated with syndecan-4 shedding could contribute to improved understanding of cardiac immune responses.

Levels of circulating syndecan-4 ectodomains are elevated in patients with acute myocardial infarction [17] and chronic heart failure [18], and although large cohort studies are lacking, syndecan-4 has been suggested as a promising novel biomarker for risk-stratification. We recently found that along with increased mRNA expression, there are increased amounts of syndecan-4 shedding fragments in myocardial biopsies from patients with end-stage, dilated heart failure [15]. Despite these indications that syndecan-4 shedding is regulated in cardiac pathology, the function of this post-translational modification has to our knowledge not been studied in the diseased heart. Here we build on our previous observation that syndecan-4 shedding is increased by LPS in cardiac myocytes and fibroblasts in culture [15], and explored the functional role of syndecan-4 shedding *in vivo* by investigating its effects on cardiac function and immune cell recruitment using LPS challenge in mice. Shedding-induced effects on immune responses and ECM remodeling was investigated in cardiac cells *in vitro*. Although LPS challenge simulates a bacterial infection and sepsis, its receptor TLR4 also responds to endogenous ligands released during sterile immune activation in the heart [19], e.g. pressure overload and infarction, suggesting that aspects of innate immune mechanisms are shared between bacterial infections and the chronic inflammatory activation during heart failure. To confirm that syndecan-4 fragments detected in the circulation can originate from the heart, we investigated levels of syndecan-4 in blood samples obtained from the coronary sinus of patients undergoing open heart surgery.

2. Methods

A detailed description of the methods is provided in the Online Supplement.

2.1 Ethics

The study protocol for human blood sampling was reviewed and approved by the Regional Committee for Medical Research Ethics (approval number REK 290-06114), and conformed to the Declaration of Helsinki. Informed written consent was obtained from all patients. Animal experiments were reviewed and approved by the Norwegian National Animal Research Committee (ID 4325) and conformed to the Guide for the Care and Use of Laboratory Animals (NIH publication No. 85-23, revised 2011).

2.2 Human blood samples

Thirty consecutive patients operated for severe, symptomatic aortic stenosis (AS) with aortic valve replacement (AVR) at Oslo University Hospital Ullevål, Oslo, Norway, were included in this study. Blood samples were drawn during open heart surgery from a coronary sinus catheter and from the cannulated radial artery immediately after onset of cardiopulmonary bypass. Serum syndecan-4 levels were analyzed using a human syndecan-4 ELISA kit (27188, IBL, Gunma, Japan).

2.3 Mouse model of LPS challenge

Eight-ten week old male wild-type (WT) C57BL/6JBomTac (Taconic, Skensved, Denmark) and syndecan-4 knock-out (KO) mice [20] were randomized to intraperitoneal injection with a single dose of LPS (10 mg/kg, List Biological Laboratories Inc., Campbell, CA) dissolved in sterile phosphate-buffered saline (PBS) or an equivalent volume of PBS (control). Syndecan-4 KO mice were used to represent mice unable to shed syndecan-4 in response to LPS. Echocardiographic and electrocardiographic examinations and analyses including assessment of heart rate were performed before (pre-LPS) and 9 h after injections (post-LPS) by an experienced researcher blinded to genotype, on anesthetized mice breathing a mixture of 1.75% isoflurane and 98.25% O_2 on a mask, using the VEVO 2100 system (VisualSonics, Toronto, Canada), n=8. After sacrifice by cervical dislocation, hearts, lungs and kidneys were rapidly excised, LVs dissected, snap-frozen in liquid nitrogen and stored at -70°C, n=12-13. In a separate cohort, blood was drawn from the left ventricle of WT mice 9 h after LPS or PBS injection, n=9. Plasma syndecan-4 levels were analyzed using a mouse syndecan-4 ELISA kit (E03S0065, Blue Gene, Shanghai, China). Non-invasive blood pressure measurements were obtained under light anesthesia before and after LPS with a tail-cuff-based CODA system (Kent Scientific, Torrington, CT) by an experienced researcher blinded to genotype, n=5-10. Blood was drawn from the abdominal aorta to assess blood urea nitrogen (BUN) using a DetectX BUN kit (K024, Arbor Assays, Ann Arbor, MI).

2.4 HEK293 cell culture and transfection

HEK293 cells were cultured and transfected using Lipofectamine 2000 (Invitrogen, Paisley, UK) with human influenza hemagglutinin (HA)-tagged syndecan-4 in a pcDNA3.1 vector (Invitrogen; custom made by Genscript Corporation, Piscataway, NJ) and the same construct with S44/S62/S64 mutated to A44/A62/A64, as described [12]. Non-transfection or transfection with empty pcDNA3.1 vector (vehicle) served as controls. Conditioned medium was cleared by centrifugation at 5000g, and for immunoblots analyses, concentrated using Amicon Ultra-4 centrifugal filters (3 kDa cut-off, Merck Millipore, Darmstadt, Germany), n=3-6 per cell culture from three separate experiments. Conditioned medium syndecan-4 levels were analyzed using a syndecan-4 ELISA kit (27188, IBL).

2.5 Primary cultures of neonatal cardiac myocytes and fibroblasts
Primary rat cardiomyocyte and fibroblast cultures were prepared from 1-3 day old Wistar rats (Taconic) as described [15]. Following 24 h of serum deprivation, cells were stimulated with LPS (1 µg/ml, 201, List Biological Laboratories), SM7368 (10 mM, 481411, Merck Millipore) or 2 ml conditioned medium (diluted 2:1 in fresh medium) from HEK293 cells for 24 h, n=3 per cell culture from three-four separate experiments.

2.6 RNA isolation and quantitative real-time PCR (qRT-PCR)
Total RNA was isolated from LVs of mice and neonatal rat cells using RNeasy mini (74106, Qiagen Nordic, Oslo, Norway) as described [15]. Reverse transcription was performed with the iScript cDNA Synthesis Kit (Bio-Rad Laboratories, Inc., Hercules, CA). Pre-designed TaqMan assays (Applied Biosystems, Foster City, CA) were used to assess gene transcription by qRT-PCR. Results were detected on an ABI PRISM 7900HT Sequence Detection System and analyzed using the Sequence Detection System 2.3 software (Applied Biosystems).

2.7 Protein isolation and immunoblotting
LV homogenates and whole-cell protein lysates were prepared and immunoblotting performed as described [15]. For analyses of syndecan-4 protein levels, 100 µg protein were precipitated using methanol prior to treatment with HS-degrading enzymes (Heparitinase I-III and Chondritinase cABC (AMSBIO, Abingdon, UK)) as described [15]. Primary antibodies used were: anti-syndecan-4 cytoplasmic epitope (custom made, Genscript Corporation), anti-IκBα (sc-371) and anti-actin (sc-8432, Santa Cruz Biotechnology, Santa Cruz, CA), anti-p65 NF-κB (8242) and anti-HA (3724, Cell Signaling Technology, Danvers, MA). To assess shedding by immunoblotting, the transmembrane plus cytoplasmic part of syndecan-4 remaining in cells after shedding of the ectodomain was detected using an antibody recognizing a cytoplasmic epitope [12] of syndecan-4 (see Strand *et al*. [15] for details). In brief, the 10-15 kDa band represents a membrane-localized, syndecan-4-specific fragment consisting of its transmembrane and cytoplasmic domains.

2.8 HPLC
Quantification of total collagen in LVs of mice receiving LPS or PBS was obtained by analysis of LV tissue (15 µg wet weight) hydroxyproline content by high-performance liquid chromatography (HPLC).

2.9 Statistics
Data are expressed as group means ± S.E.M. Statistical analyses were performed using GraphPad Prism 5.04 and differences considered significant for $p<0.05$. Significance was determined using Mann-Whitney test, Student's paired and unpaired *t*-test or one-way ANOVA followed by Bonferroni post-hoc test, as described in figure and table legends.

3. Results

3.1 LPS induces NF-κB-dependent syndecan-4 expression and shedding from cardiac myocytes and fibroblasts *in vivo* and *in vitro*

Nine h after intraperitoneal injection of LPS (10 mg/kg) in WT mice, LV syndecan-4 mRNA was increased 9.8-fold compared to PBS-injected controls (Fig. 1A). LV protein lysates treated with HS-degrading enzymes showed no increase in full-length syndecan-4 (Fig. 1B), consistent with the majority of LPS-induced syndecan-4 being shed. We have previously, through a number of experiments, identified that syndecan-4 shedding from cells can be assessed by quantification of the 10-15 kDa syndecan-4 fragment (syndecan-4 transmembrane plus cytoplasmic domain; Fig. 1C) remaining in cells after shedding of the ectodomain [15]. In line with LPS-induced shedding of syndecan-4 in the myocardium, levels of the cellular fragment was increased 30-fold in LVs of mice injected with LPS (Fig. 1B, lower panel), and levels of shed syndecan-4 in blood collected from the LV increased 3-fold (4.80±1.28 in LPS vs. 1.60±0.49 ng/ml in controls) (Fig. 1D). Similar to our previous findings from cultured cardiac myocytes and fibroblasts [15], syndecan-4 mRNA was elevated 3.7- and 9-fold in neonatal rat myocyte and fibroblast cultures treated with LPS for 24 h, respectively (Fig. 1E, F). The increased expression was blocked by co-treatment with the NF-κB inhibitor SM7368, showing that LPS-induced syndecan-4 expression was NF-κB dependent. Similar to in mouse ventricles, LPS induced no change in full-length syndecan-4 in cultured cardiac myocytes and fibroblasts (Fig. 1G, H), with levels of the cellular fragment increasing 5.6- and 23-fold in the two cardiac cell types, respectively (Fig. 1G, H, lower panel). Confirming LPS-induced syndecan-4 shedding in cardiac cells *in vitro* also after 9 h of LPS challenge, comparable to our *in vivo* results, the cellular syndecan-4 fragment was increased 4.3- and 13-fold in cardiac myocytes and fibroblasts (Supplemental Fig. S1A, B). Syndecan-4 shedding was attenuated by co-treatment with LPS and the NF-κB inhibitor SM7368 (Fig. 1I, J), showing that increased shedding as well as expression of syndecan-4 was NF-κB dependent. Increased levels of the p65 subunit of NF-κB and reduced levels of inhibitor of κB (IκB)α confirmed activation of NF-κB in cardiac myocytes and fibroblasts after LPS (Supplemental Fig. S2A, B). The TLR4 inhibitor CLI-095 blocked LPS-induced syndecan-4 mRNA, indicating TLR4-mediated syndecan-4 expression in cardiac cells in response to LPS (Supplemental Fig. S3A, B).

Enzymes proposed by others to mediate shedding of syndecan-4 ectodomains include matrix metalloproteinase (MMP)2 and 9, a disintegrin and metalloproteinase (ADAM)17 and ADAMs with thrombospondin motifs (ADAMTS)1 and 4 [5]. Following *in vivo* LPS challenge, LV expression of ADAMTS1 (Fig. 2A), ADAMTS4 (Fig. 2B) and MMP9 (Fig. 2C) was increased. Remarkably, LPS induced a 46-fold increase in ADAMTS4 mRNA (Fig. 2B). MMP2 expression was reduced after LPS (Fig. 2D) and we observed no change in ADAM17 mRNA levels (Fig. 2E). In cardiac myocytes and fibroblasts *in vitro*, LPS had little effect on ADAMTS1, but increased the expression of ADAMTS4, MMP9, MMP2 and ADAM17 (Supplemental Fig. S4A-J). Thus, it is likely that ADAMTS1, ADAMTS4 and MMP9 are involved in syndecan-4 ectodomain shedding in hearts in response to LPS.

These data suggested that in response to LPS, syndecan-4 expression and ectodomain shedding are substantially elevated in the heart through an NF-κB-dependent mechanism. Importantly, as increased syndecan-4 expression did not result in increased full-length protein, but rather increased shedding, LPS challenge constituted a model to study effects of syndecan-4 shedding in the heart *in vivo*, isolated from altered syndecan-4 full-length levels. Since LPS resulted in robust upregulation of syndecan-4 shedding without altering full-length protein, responses to LPS in syndecan-4 KO mice were interpreted as resulting mainly from the inability to shed syndecan-4.

3.2 Mice unable to shed syndecan-4 show exacerbated cardiac dysfunction in response to LPS

To understand whether increased syndecan-4 shedding was important for heart function after LPS, echocardiograms and electrocardiograms of syndecan-4 KO mice were analyzed 9 h after injection of LPS and compared to those of WT controls. Before injections, syndecan-4 KO and WT mice had similar echocardiographic characteristics (pre-LPS values, Table I) and blood pressures (Supplemental Table SI), and no mortality was observed throughout the experiment. Severe cardiovascular dysfunction was evident after 9 h of LPS (post-LPS values, Tables I and SI), characterized by reduced blood pressure and heart rate, increased lung weight, and lower myocardial tissue velocities and reduced LV dimensions in diastole i.e. LV internal diameter in diastole (LVIDd) and end-diastolic volume (EDV; Fig. 3A) compared with pre-LPS values or PBS controls, with no differences in these parameters between WT and syndecan-4 KO mice. Syndecan-4 KO mice exerted lower ejection fraction (EF; Fig. 3B, C) and lower diastolic tissue velocity (Fig. 3D) than WT, indicating aggravated cardiac dysfunction in syndecan-4 KO mice after LPS challenge. M-mode recordings of the LV indicated presence of less synchronous contraction in syndecan-4 KO mice compared to WT, i.e. septal-to-posterior wall motion delay (SPWMD; Table I) and prolonged QRS duration (Fig. 3E) as indication of LPS-induced electrical dysfunction. Although it failed to reach statistical significance, there was a tendency for higher BNP expression in syndecan-4 KO hearts after LPS (8.3- vs. 5.5-fold in WT compared to respective PBS controls, $p=0.12$).

LPS induced kidney dysfunction and injury, evidenced by increased levels of BUN (Supplemental Fig. S5A) and mRNA expression of markers of kidney injury [21], i.e. kidney injury molecule (KIM)-1 and neutrophil gelatinase associated lipocalin (NGAL) (Supplemental Fig. S5B, C). BUN was increased to the same extent in WT and syndecan-4 KO mice, indicating that exacerbated kidney dysfunction was not responsible for the aggravated cardiac response observed in mice lacking syndecan-4.

Thus, in syndecan-4 KO mice which are unable to shed syndecan-4, we observed exacerbated cardiac dysfunction associated with a pathological contractile pattern in response to LPS, indicating that syndecan-4 shedding mitigates primary cardiac dysfunction after LPS challenge.

3.3 Mice unable to shed syndecan-4 show reduced recruitment of immune cells to the myocardium in response to LPS

We hypothesized that the exacerbated cardiac dysfunction in mice unable to shed syndecan-4 (syndecan-4 KO mice) in response to LPS was associated with impaired immune cell recruitment to the heart. Nine h after LPS injection, expression of CD8, a receptor on cytotoxic T-cells, was increased 2.7-fold in WT hearts compared to PBS controls (Fig. 4A). Interestingly, CD8 levels were significantly lower in syndecan-4 KO mice after LPS, suggesting that syndecan-4 shedding was important for recruitment of cytotoxic T-cells to the heart. Levels of the pan-T-cell receptor CD3 (Fig. 4B) and the T-helper cell-specific CD4 (Fig. 4C) were reduced to a similar extent in WT and syndecan-4 KO mice challenged with LPS, compared to respective PBS controls. Recruitment of other immune cells to the heart was also affected in syndecan-4 KO mice, evidenced by attenuated LV expression of a marker expressed on all leukocytes, i.e. CD11a (Fig. 4D), and a macrophage marker, F4/80 (Fig. 4E), in syndecan-4 KO mice.

LPS is well-known to induce IL-1β and TNFα [16]. To exclude that the reduced recruitment of immune cells to the myocardium of syndecan-4 KO mice was secondary to an impaired cytokine response, TNFα and IL-1β expression was compared among the two genotypes after LPS. We confirmed no difference in TNFα or IL-1β levels (Fig. 4F, G). Thus, syndecan-4 KO mice unable to shed syndecan-4 in response to LPS demonstrated an impaired

recruitment of immune cells to the myocardium, and in particular, reduced recruitment of cytotoxic T-cells.

3.4 Shed syndecan-4 ectodomains regulate receptors for immune cell recruitment and activate innate immune signaling in cardiac myocytes and fibroblasts *in vitro*

Intercellular adhesion molecule (Icam)1 and vascular cell adhesion molecule (Vcam)1 are critically involved in regulating immune cell recruitment and infiltration to tissues during inflammation [22]. We hypothesized that shed syndecan-4 ectodomains regulate immune cell recruitment through induction of adhesion molecules on cardiac cells. To test our hypothesis, we capitalized on the constitutive shedding of syndecan-4 after its overexpression in cells [15], confirmed by increased levels of the cellular syndecan-4 fragment (Fig. 5A) and detection of shed ectodomains in the medium of HEK293 cells (Fig. 5B, C). Conditioned medium containing the shed syndecan-4 ectodomains was applied to cardiac myocytes and fibroblasts in culture, with medium from non-transfected or cells transfected with an empty vector (vehicle) serving as controls. Interestingly, and consistent with regulation of immune cell adhesion molecules by shed syndecan-4 ectodomains, cardiac myocytes and fibroblasts treated with the syndecan-4 conditioned medium responded with increased expression of Icam1 (Fig. 5D, F) and Vcam1 (Fig. 5E, G). Of notice, Vcam1 mRNA was increased 120-fold in cardiac fibroblasts. Conditioned medium from HEK293 cells overexpressing syndecan-4 with mutated HS attachment sites (syn-4 ΔHS) failed to induce a transcriptional response in cardiac cells, indicating that the HS GAG chains were essential for this effect of shed syndecan-4. To study whether increased levels of shed syndecan-4 ectodomains also activated other central components of innate immunity signaling in cardiac cells, levels of TNFα, IL-1β and NF-κB activation were assessed. Both cardiac myocytes and fibroblasts showed increased TNFα (Fig. 5H, J) and IL-1β (Fig. 5I, K) mRNA. Increased levels of p65 NF-κB and reduced levels of IκBα in cardiac myocytes (Fig. 5L) and fibroblasts (Fig. 5M) treated with syndecan-4 conditioned medium were consistent with NF-κB activation. Since a number of soluble proteoglycans have been shown to activate TLR4 [23], we tested whether this receptor was involved in shed syndecan-4-mediated signaling. Co-treatment with the TLR4 inhibitor CLI-095 did not reduce levels of Icam1 (Supplemental Fig. S6A, E), Vcam1 (Supplemental Fig. S6B, F), TNFα (Supplemental Fig. S6C, G) or IL-1β (Supplemental Fig. S6D, H) in cardiac myocytes or fibroblasts, respectively, suggesting that the shed ectodomain of syndecan-4 does not function via TLR4. Finally, expression of Icam1 (Fig. 5N) and Vcam1 (Fig. 5O) was attenuated in syndecan-4 KO hearts after LPS, supporting our finding of reduced recruitment of immune cells to syndecan-4 KO hearts unable to shed syndecan-4. Thus, shed syndecan-4 ectodomains elevated expression of immune cell adhesion molecules and activated the innate immunity NF-κB signaling cascade in myocytes and fibroblasts of the heart.

3.5 Shed syndecan-4 ectodomains regulate ECM remodeling in cardiac fibroblasts *in vitro*

We have identified that syndecan-4, when upregulated in pressure-overloaded hearts, regulates cardiac function by determining myofibroblast differentiation, collagen production, and amounts and activity of the collagen cross-linking enzyme lysyl oxidase (LOX) [14, 24]. We hypothesized that these properties of cardiac fibroblasts were affected by shedding of syndecan-4. In contrast to pressure overload, fibroblast function was suppressed by LPS treatment, shown by lower expression of the myofibroblast signature gene smooth muscle α-actin (α-SMA; Fig. 6A), collagen I (Fig. 6B) and III (Fig. 6C) and the proliferation marker proliferating cell nuclear antigen (PCNA; Fig. 6D) in cardiac fibroblast cell cultures. Similar alterations were found after LPS challenge *in vivo*: reduced expression of α-SMA (Fig. 6E),

collagen I (Fig. 6F) and III (Fig. 6G). Although collagen expression was downregulated, we could not over this short time-span of 9 h, as expected, detect any difference in total collagen protein (Fig. 6H). Interestingly, LPS increased expression of LOX 3.3-fold in cardiac fibroblasts *in vitro* (Fig. 6I) and 4.5-fold in LVs *in vivo* (Fig. 6J), suggesting that LPS induced alterations in collagen matrix quality. Furthermore, increased expression of LOX (Fig. 6K) and reduced mRNA (Fig. 6L, M) of collagen I and III were observed in cardiac fibroblasts exposed to shed syndecan-4 ectodomains, suggesting that shed syndecan-4 fragments could mediate these effects of LPS.

Consistent with a role for shed syndecan-4 in ECM remodeling, expression of several ECM molecules in cardiac fibroblasts was altered by increased levels of syndecan-4 ectodomains, including members of the MMPs, i.e. MMP2 and 9 (Fig. 6N-Q), TIMPs, i.e. TIMP1, 3 and 4 (Fig. 6R-U), small leucine-rich proteoglycans (SLRPs), i.e. decorin, fibromodulin and lumican (Supplemental Fig. S7A-D) and hyaluronan synthases, i.e. Has1 (Supplemental Fig. S7E-F). Importantly, increased expression of MMP2 and 9 and reduced expression TIMP3 and 4 indicated that shed syndecan-4 shifted the MMP/TIMP balance towards ECM degradation. Accordingly, the ratio of MMP2 to TIMP3 and TIMP4 was increased 16.8- ($P<0.05$) and 2.4-fold ($P<0.001$), and the ratio of MMP9 to TIMP3 and TIMP4 was increased 59.6- ($P<0.05$) and 8.9-fold ($P<0.001$), respectively, in cardiac fibroblasts exposed to shed syndecan-4 compared to controls.

To investigate whether shed syndecan-4 ectodomains could influence on cardiac cell growth, markers of hypertrophy, i.e. alpha skeletal muscle actin (Acta1), and proliferation, i.e. PCNA, were assessed in cardiac myocytes and fibroblasts, respectively, exposed to increased levels of shed syndecan-4. Interestingly, both markers were reduced (Fig. 6V, W) suggesting that shed syndecan-4 inhibited cardiac cell growth of both cardiomyocytes and cardiac fibroblasts.

3.6 Syndecan-4 is shed the from human hearts

Finally, we investigated whether syndecan-4 could be shed from human hearts. We measured syndecan-4 levels in blood samples from the coronary sinus, which collects venous blood from the myocardium, and compared them to levels in the radial artery of the same patient, in aortic stenosis patients undergoing aortic valve replacement surgery (see Table SII for patient characteristics). Consistent with syndecan-4 being shed from the human heart, circulating syndecan-4 levels were 2.8-fold higher in the coronary sinus (14.95±3.33 vs. 9.83±2.51 ng/ml in the radial artery) (Fig. 7).

4. Discussion

The present work investigates effects of ectodomain shedding of the transmembrane HS proteoglycan syndecan-4 and demonstrates for the first time consequences of this process in mediating innate immune responses and ECM remodeling in the heart. LPS challenge in mice increased cardiac syndecan-4 expression and shedding without increasing full-length protein, suggesting that the majority of LPS-induced syndecan-4 protein was shed *in vivo* and thus that lack of shedding was the major mechanism responsible for the altered LPS response observed in syndecan-4 KO mice. A parallel upregulation of ADAMTS1, ADAMTS4 and MMP9 suggested these sheddase enzymes to regulate LPS-mediated syndecan-4 shedding in the ECM of the heart. Syndecan-4 KO mice, unable to shed syndecan-4 in response to LPS, showed exacerbated LV dysfunction, suggesting that syndecan-4 shedding mitigates cardiac dysfunction after LPS. The impaired cardiac function of syndecan-4 KO mice in response to LPS was paralleled by attenuated immune cell recruitment, in particular of cytotoxic T-cells. In cultured cardiac myocytes and fibroblasts, shed syndecan-4 ectodomains upregulated receptors for immune cell adhesion and activated innate immunity signaling. Shed syndecan-4 regulated expression of ECM molecules associated with collagen synthesis, cross-linking and turnover in cardiac fibroblasts, indicating that syndecan-4 shedding affected ECM remodeling. Finally, syndecan-4 was shed from human hearts, evidenced by higher levels of syndecan-4 ectodomains in serum from the coronary sinus obtained during open heart surgery, compared to levels in the radial artery.

At present, effects of syndecan-4 shedding and in what etiologies and stages of cardiac dysfunction it occurs, remain unknown. We investigated syndecan-4 shedding in an experimental model where the majority of upregulated syndecan-4 was shed in order to isolate the shedding process and its effects from those of increased syndecan-4 full-length levels. In cultured cardiomyocytes and fibroblasts *in vitro* as well as in WT mice *in vivo*, LPS increased cardiac syndecan-4 expression and shedding without altering full-length levels. Importantly, we showed that in syndecan-4 KO mice after LPS, left ventricular dysfunction was exacerbated, indicating that syndecan-4 shedding mitigated cardiac dysfunction after LPS. Although it is likely that the inability to shed syndecan-4 represents the major mechanism responsible for the different LPS response in syndecan-4 KO mice, we cannot exclude an effect of lack of the full-length molecule. We did not observe higher mortality in syndecan-4 KO mice after LPS, as previously reported [25], however the reduced ventricular function was in line with an aggravated response. Similarly, in a model of acute pneumonia, syndecan-4 shedding was elevated in WT mice and syndecan-4 KO mice had increased mortality, suggesting a protective role for syndecan-4 shedding in acute bacterial pneumonia [26].

A role for syndecan-4 in cardiac pathology of various etiologies has been reported by us and others. In infarcted and pressure-overloaded hearts, syndecan-4 mRNA and full-length protein is upregulated and believed to regulate hypertrophic [12, 27] and fibrotic [14, 24] remodeling via regulation of calcineurin-NFAT signaling through its cytoplasmic domain. Syndecan-4 KO mice show more cardiac ruptures, reduced inflammation and granulation tissue formation after myocardial infarction [13]. In line with this, intramyocardial administration of a virus carrying full-length syndecan-4 results in reduced mortality and improved cardiac function in infarcted rat hearts [28]. Overexpression of syndecan-4 triggers constitutive shedding [15], also confirmed here in HEK293 cells. Thus, it is possible that altered shedding together with altered full-length levels contribute to the syndecan-4-dependent responses to infarction and pressure overload. After infarction, adenoviral administration of the syndecan-4 ectodomain into the circulation of mice resulted in increased mortality due to cardiac rupture, similar to what was observed in syndecan-4 KO mice [13]. Thus, effects of syndecan-4 shedding in the heart are likely etiology-specific and dependent

on whether the immune activation is chronic, as in heart failure models, or acute and responding to a bacterial infection, as in the LPS model.

In this study we build on our previous *in vitro* findings to show that induction of syndecan-4 expression and subsequent shedding in the heart is a response to LPS, substantiating that syndecan-4 shedding is an effector of the innate immune system *in vivo*. The innate immune response limits the extent of injury and facilitates tissue repair after insults, and its sustained activation is deleterious in chronic etiologies, including heart failure [2, 19]. It is activated by pattern recognition receptors (PRRs) responding to pathogen- or damage-associated molecular patterns (PAMPs or DAMPs). LPS is a well-known PAMP activating innate immune signaling through TLR4. A role for proteoglycans as endogenous DAMPs during sterile inflammation is emerging, suggesting they activate PRRs during tissue stress and injury [23]. To date, ECM-localized proteoglycans such as biglycan, decorin and versican [29-31] and GAG fragments [32, 33] have been implicated in this process. Here we show for the first time that shed syndecan-4 can act as a DAMP, activating innate immunity pathways, e.g. NF-κB signaling and enhanced TNFα and IL-1β expression. Thus, the shed ectodomains of syndecan-4 may contribute to elevated levels of TNFα and IL-1β in the heart. Since LPS is a potent inducer of these cytokines from numerous sources *in vivo,* it is likely that the contribution from shed syndecan-4 was too minor to be detected *in vivo.* We found that the HS chains of shed syndecan-4 were essential for inducing signaling in cardiac cells. However, although TLR4 has been shown to respond to HS fragments [33], our observations did not support a role for TLR4 in shed syndecan-4-mediated signaling, suggesting other PRRs or mechanisms are involved.

We show here that increased syndecan-4 expression and shedding after LPS affects expression of crucial immune cell adhesion receptors, i.e. Icam1 and Vcam1, in cardiac fibroblasts and myocytes. The central role of these molecules is well established, e.g. Icam1 KO mice display impaired immune cell migration to inflammatory sites [34, 35]. Thus, our findings offer a novel mechanism whereby syndecan-4 shedding regulates recruitment of immune cells to the heart. We observed reduced expression of the pan-immune cell marker CD11a, which is known to interact with Icam1 [36], in addition to markers consistent with cytotoxic T-cells and macrophages, in syndecan-4 KO hearts after LPS. These results suggested that syndecan-4 shedding regulated cardiac immune cell recruitment, and could explain the observed reduction in T-cell and macrophage recruitment to syndecan-4 KO hearts after pressure overload [15] and infarction [13]. There is strong evidence suggesting that immune cells, and in particular T-cells, are central in cardiac pathogenesis. T-cells impact on cardiomyocyte function and remodeling [37] and fibroblast-mediated changes in ECM structure and composition [38, 39]. Thus, the reduced T-cell recruitment observed in syndecan-4 KO hearts likely contributed to the observed dysfunction after LPS. Our finding of reduced cardiac macrophage recruitment after LPS is of unknown importance to the observed dysfunction, as the opposite, i.e. increased numbers of cardiac macrophages have been associated with dysfunction after LPS [40]. However, our results are consisted with a previous report showing LPS-induced macrophage apoptosis [41].

During infection and inflammation, recruitment of immune cells goes hand in hand with ECM remodeling. Degradation of collagens has been observed in several cells and tissues after LPS challenge [42, 43], and our findings of reduced cardiac fibroblast activation and collagen production after LPS are in line with these observations. Interestingly, these effects could be mediated by shed syndecan-4 ectodomains. Our results indicate that inflammation-induced syndecan-4 shedding attenuates, and opposes, the effects of full-length syndecan-4, which we have previously shown to upregulate pro-fibrotic signaling and collagen production in the pressure-overloaded heart [14]. We found that expression of LOX was increased by LPS and shed syndecan-4. LOX is crucial in maintaining collagen matrix

stability and is believed to be a key determinant of myocardial stiffness. Whether this LPS-induced LOX upregulation increases stiffness of the heart needs further investigation, however a similar response has been noted in mouse lungs *in vivo* [44] and in endothelial cells in *vitro* [45], where LPS upregulated LOX expression. This was associated with increased lung stiffness, reduced compliance and increased vascular permeability. LOX has also been found to be a chemotactic for monocytes [46], and thus we speculate that it could contribute to the immune cell recruitment mediated by shed syndecan-4. In addition to modulating collagen production and cross-linking, we showed that shed syndecan-4 fragments regulated expression of several important ECM molecules, e.g. MMPs, TIMPs and SLRPs in cardiac fibroblasts. Importantly, shed syndecan-4 shifted the MMP/TIMP balance towards ECM degradation, suggesting that inflammation-induced syndecan-4 shedding may have profound effects on ECM remodeling, and thus, cardiac function.

Studies in relatively small patient cohorts have shown that circulating levels of syndecan-4 are elevated in patients with acute myocardial infarction [17] and chronic heart failure [18]. In heart failure patients, serum syndecan-4 correlates positively with LV geometrical parameters and negatively with EF, suggesting syndecan-4 as a biomarker of remodeling with potential for risk-stratification [18, 47]. Since heart failure is a multi-organ syndrome, the source of the soluble syndecan-4 ectodomains detected in the circulation of heart failure patients could be a number of cell types and tissues. In the present work, we determined that syndecan-4 can indeed be shed from the heart into the circulation by comparing syndecan-4 levels in blood from the coronary sinus to that of the radial artery in aortic stenosis patients. This is interesting in view of our previous report on increased syndecan-4 mRNA and full-length protein in myocardial biopsies from aortic stenosis patients taken per-operatively [12]. Thus, the increased circulating syndecan-4 measured in patients with cardiac pathology could at least in part, originate from the heart, consistent with our previous observation of more syndecan-4 shedding fragments in myocardial biopsies from explanted hearts of patients with end-stage, dilated heart failure [15]. Moreover, based on our LPS mouse model with increased syndecan-4 shedding that can be detected in blood, we speculate that circulating syndecan-4 might be explored as a biomarker in patients with sepsis. At present, many functional aspects of increased circulating syndecan-4 remains unresolved. However, since syndecans bind a multitude of growth factors and cytokines via their HS chains, it is plausible that shed syndecan-4 acts as a circulating reservoir of signaling molecules, capable of inducing responses distant from where they originated.

In conclusion, shedding of syndecan-4 ectodomains is part of the innate immune response of the heart. Shed syndecan-4 ectodomains act on cardiac myocytes and fibroblasts, inducing innate immunity signaling, promoting immune cell recruitment and collagen matrix remodeling. Syndecan-4 shedding likely represents a mechanism in which cells tune tissue inflammation to bacterial infections, however when chronically activated, contributes to cardiac remodeling and dysfunction. Increased levels of shed syndecan-4 in the circulation of heart failure patients likely reflects increased inflammation and could originate from the heart.

Funding
This work was supported by the Research Council of Norway, Stiftelsen Kristian Gerhard Jebsen, Anders Jahre's Fund for the Promotion of Science, the South-Eastern Regional Health Authority, Ullevålfondet, Norway, and the Simon Fougner Hartmanns Family Fund, Denmark.

Disclosures
None.

Acknowledgements
We are deeply grateful to patients and staff at the department of surgery and staff at the animal facility at Oslo University Hospital, Oslo, Norway. We are grateful to Bjørg Ausbø, Marita Martinsen, Hilde Dishington and Almira Hasic for technical assistance, and to Dr. Sarah A. Wilcox-Adelman for donating the syndecan-4 KO mice.

References

[1] Frangogiannis NG. The inflammatory response in myocardial injury, repair, and remodelling. Nat Rev Cardiol. 2014;11:255-65.
[2] Yndestad A, Damås JK, Øie E, Ueland T, Gullestad L, Aukrust P. Role of inflammation in the progression of heart failure. Curr Cardiol Rep. 2007;9:236-41.
[3] Heymans S, Hirsch E, Anker SD, Aukrust P, Balligand J-L, Cohen-Tervaert JW, et al. Inflammation as a therapeutic target in heart failure? A scientific statement from the Translational Research Committee of the Heart Failure Association of the European Society of Cardiology. Eur J Heart Fail. 2009;11:119-29.
[4] Götte M. Syndecans in inflammation. FASEB J. 2003;17:575-91.
[5] Manon-Jensen T, Itoh Y, Couchman JR. Proteoglycans in health and disease: the multiple roles of syndecan shedding. FEBS J. 2010;277:3876-89.
[6] Lambaerts K, Wilcox-Adelman SA, Zimmermann P. The signaling mechanisms of syndecan heparan sulfate proteoglycans. Curr Opin Cell Biol. 2009;21:662-9.
[7] Couchman JR. Transmembrane signaling proteoglycans. Annu Rev Cell Dev Biol. 2010;26:89-114.
[8] Li Q, Park PW, Wilson CL, Parks WC. Matrilysin shedding of syndecan-1 regulates chemokine mobilization and transepithelial efflux of neutrophils in acute lung injury. Cell. 2002;111:635-46.
[9] Kainulainen V, Wang H, Schick C, Bernfield M. Syndecans, heparan sulfate proteoglycans, maintain the proteolytic balance of acute wound fluids. J Biol Chem. 1998;273:11563-9.
[10] Subramanian SV, Fitzgerald ML, Bernfield M. Regulated shedding of syndecan-1 and -4 ectodomains by thrombin and growth factor receptor activation. J Biol Chem. 1997;272:14713-20.
[11] Finsen AV, Woldbaek PR, Li J, Wu J, Lyberg T, Tønnessen T, et al. Increased syndecan expression following myocardial infarction indicates a role in cardiac remodeling. Physiol Genomics. 2004;16:301-8.
[12] Finsen AV, Lunde IG, Sjaastad I, Østli EK, Lyngra M, Jarstadmarken HO, et al. Syndecan-4 is essential for development of concentric myocardial hypertrophy via stretch-induced activation of the calcineurin-NFAT pathway. PLoS ONE. 2011;6:e28302.
[13] Matsui Y, Ikesue M, Danzaki K, Morimoto J, Sato M, Tanaka S, et al. Syndecan-4 prevents cardiac rupture and dysfunction after myocardial infarction. Circ Res. 2011;108:1328-39.
[14] Herum KM, Lunde IG, Skrbic B, Florholmen G, Behmen D, Sjaastad I, et al. Syndecan-4 signaling via NFAT regulates extracellular matrix production and cardiac myofibroblast differentiation in response to mechanical stress. J Mol Cell Cardiol. 2013;54:73-81.
[15] Strand ME, Herum KM, Rana ZA, Skrbic B, Askevold ET, Dahl CP, et al. Innate immune signaling induces expression and shedding of the heparan sulfate proteoglycan syndecan-4 in cardiac fibroblasts and myocytes, affecting inflammation in the pressure-overloaded heart. FEBS J. 2013;280:2228-47.
[16] Alexander C, Rietschel ET. Invited review: bacterial lipopolysaccharides and innate immunity. J Endotoxin Res. 2001;7:167-202.
[17] Kojima T, Takagi A, Maeda M, Segawa T, Shimizu A, Yamamoto K, et al. Plasma levels of syndecan-4 (ryudocan) are elevated in patients with acute myocardial infarction. Thromb Haemost. 2001;85:793-9.
[18] Takahashi R, Negishi K, Watanabe A, Arai M, Naganuma F, Ohyama Y, et al. Serum syndecan-4 is a novel biomarker for patients with chronic heart failure. J Cardiol. 2011;57:325-32.
[19] Mann DL. The emerging role of innate immunity in the heart and vascular system: for whom the cell tolls. Circ Res. 2011;108:1133-45.
[20] Echtermeyer F, Streit M, Wilcox-Adelman S, Saoncella S, Denhez F, Detmar M, et al. Delayed wound repair and impaired angiogenesis in mice lacking syndecan-4. J Clin Invest. 2001;107:R9-R14.
[21] Vaidya VS, Ferguson MA, Bonventre JV. Biomarkers of acute kidney injury. Annu Rev Pharmacol Toxicol. 2008;48:463-93.
[22] Ley K. Molecular mechanisms of leukocyte recruitment in the inflammatory process. Cardiovasc Res. 1996;32:733-42.
[23] Frey H, Schroeder N, Manon-Jensen T, Iozzo RV, Schaefer L. Biological interplay between proteoglycans and their innate immune receptors in inflammation. FEBS J. 2013;280:2165-79.
[24] Herum KM, Lunde IG, Skrbic B, Louch WE, Hasic A, Boye S, et al. Syndecan-4 is a key determinant of collagen cross-linking and passive myocardial stiffness in the pressure-overloaded heart. Cardiovasc Res. 2015;106:217-26.
[25] Ishiguro K, Kadomatsu K, Kojima T, Muramatsu H, Iwase M, Yoshikai Y, et al. Syndecan-4 deficiency leads to high mortality of lipopolysaccharide-injected mice. J Biol Chem. 2001;276:47483-8.
[26] Nikaido T, Tanino Y, Wang X, Sato S, Misa K, Fukuhara N, et al. Serum syndecan-4 as a possible biomarker in patients with acute pneumonia. J Infect Dis. 2015;Epub ahead of print.
[27] Echtermeyer F, Harendza T, Hubrich S, Lorenz A, Herzog C, Mueller M, et al. Syndecan-4 signalling inhibits apoptosis and controls NFAT activity during myocardial damage and remodelling. Cardiovasc Res. 2011;92:123-31.

[28] Xie J, Wang J, Li R, Dai Q, Yong Y, Zong B, et al. Syndecan-4 over-expression preserves cardiac function in a rat model of myocardial infarction. J Mol Cell Cardiol. 2012;53:250-8.
[29] Schaefer L, Babelova A, Kiss E, Hausser H-J, Baliova M, Krzyzankova M, et al. The matrix component biglycan is proinflammatory and signals through Toll-like receptors 4 and 2 in macrophages. J Clin Invest. 2005;115:2223-33.
[30] Merline R, Moreth K, Beckmann J, Nastase MV, Zeng-Brouwers J, Tralhão JG, et al. Signaling by the matrix proteoglycan decorin controls inflammation and cancer through PDCD4 and microRNA-21. Sci Signal. 2011;4:ra75.
[31] Kim S, Takahashi H, Lin W-W, Descargues P, Grivennikov S, Kim Y, et al. Carcinoma-produced factors activate myeloid cells through TLR2 to stimulate metastasis. Nature. 2009;457:102-6.
[32] Noble PW, McKee CM, Cowman M, Shin HS. Hyaluronan fragments activate an NF-kappa B/I-kappa B alpha autoregulatory loop in murine macrophages. J Exp Med. 1996;183:2373-8.
[33] Johnson GB, Brunn GJ, Kodaira Y, Platt JL. Receptor-mediated monitoring of tissue well-being via detection of soluble heparan sulfate by toll-like receptor 4. J Immunol. 2002;168:5233-9.
[34] Yang L, Froio RM, Sciuto TE, Dvorak AM, Alon R, Luscinskas FW. ICAM-1 regulates neutrophil adhesion and transcellular migration of TNF-α-activated vascular endothelium under flow. Blood. 2005;106:584-92.
[35] Sligh JE, Ballantyne CM, Rich SS, Hawkins HK, Smith CW, Bradley A, et al. Inflammatory and immune responses are impaired in mice deficient in intercellular adhesion molecule 1. Proc Natl Acad Sci. 1993;90:8529-33.
[36] Shimaoka M, Xiao T, Liu J-H, Yang Y, Dong Y, Jun C-D, et al. Structures of the αL I domain and its complex with ICAM-1 reveal a shape-shifting pathway for integrin regulation. Cell. 2003;112:99-111.
[37] Binah O. Cytotoxic lymphocytes and cardiac electrophysiology. J Mol Cell Cardiol. 2002;34:1147-61.
[38] Yu Q, Vazquez R, Zabadi S, Watson RR, Larson DF. T-lymphocytes mediate left ventricular fibrillar collagen cross-linking and diastolic dysfunction in mice. Matrix Biol. 2010;29:511-8.
[39] Hofmann U, Beyersdorf N, Weirather J, Podolskaya A, Bauersachs J, Ertl G, et al. Activation of CD4+ T lymphocytes improves wound healing and survival after experimental myocardial infarction in mice. Circulation. 2012;125:1652-63.
[40] Deleon-Pennell KY, de Castro Brás LE, Lindsey ML. Circulating Porphyromonas gingivalis lipopolysaccharide resets cardiac homeostasis in mice through a matrix metalloproteinase-9-dependent mechanism. Physiological Reports. 2013;1:e00079.
[41] Hsu L-C, Park JM, Zhang K, Luo J-L, Maeda S, Kaufman RJ, et al. The protein kinase PKR is required for macrophage apoptosis after activation of Toll-like receptor 4. Nature. 2004;428:341-5.
[42] Wendremaire M, Mourtialon P, Goirand F, Lirussi F, Barrichon M, Hadi T, et al. Effects of leptin on lipopolysaccharide-induced remodeling in an in vitro model of human myometrial inflammation. Biol Reprod. 2013;88:45, 1-10.
[43] Wahl LM, Wahl SM, Mergenhagen SE, Martin GR. Collagenase Production by Endotoxin-Activated Macrophages. Proc Natl Acad Sci. 1974;71:3598-601.
[44] Mammoto A, Mammoto T, Kanapathipillai M, Wing Yung C, Jiang E, Jiang A, et al. Control of lung vascular permeability and endotoxin-induced pulmonary oedema by changes in extracellular matrix mechanics. Nat Commun. 2013;4:1759.
[45] Mambetsariev I, Tian Y, Wu T, Lavoie T, Solway J, Birukov KG, et al. Stiffness-activated GEF-H1 expression exacerbates LPS-induced lung inflammation. PLoS ONE. 2014;9:e92670.
[46] Lazarus HM, Cruikshank WW, Narasimhan N, Kagan HM, Center DM. Induction of human monocyte motility by lysyl oxidase. Matrix Biol. 1995;14:727-31.
[47] Bielecka-Dabrowa A, von Haehling S, Aronow WS, Ahmed MI, Rysz J, Banach M. Heart failure biomarkers in patients with dilated cardiomyopathy. Int J Cardiol. 2013;168:2404-10.

Tables

Table I Characteristics of syndecan-4 KO and WT mice after LPS challenge

	Pre-LPS		Post-LPS		Post-PBS	
	WT	**Syn-4KO**	**WT**	**Syn-4KO**	**WT**	**Syn-4KO**
N			13	13	12	12
Biometric data						
Post-LPS BW (g)			27.18±0.63	25.48±0.35**#	27.18±0.67	27.28±0.32
LVW/BW (mg/g)			3.27±0.08	3.76±0.24	3.29±0.07	3.41±0.07
LW/BW (mg/g)			6.85±0.30**	6.51±0.24*	5.73±0.20	5.92±0.14
LV mRNA expression						
BNP/Rpl4 (AU)			5.54±1.17**	8.26±0.80***	1.00±0.20	1.00±0.18
N	8	8	8	8		
Electrocardiography						
Heart rate (BPM)	467.30±6.63	475.90±16.63	391.10±16.45**	368.90±9.07***	N/A	N/A
QRS-duration (ms)	10.99±0.31	11.30±0.31	19.49±0.79***	22.78±0.82***#	N/A	N/A
QT interval (ms)	36.15±0.85	36.72±1.22	73.95±0.90***	81.66±2.28***##	N/A	N/A
QTc interval (ms)	100.9±2.58	103.1±2.68	188.8±3.09***	202.1±4.99***#	N/A	N/A
M-mode echocardiography						
LAD (mm)	1.77±0.04	1.78±0.01	1.87±0.07	1.89±0.06	N/A	N/A
LVPWd (mm)	0.68±0.01	0.69±0.02	0.70±0.01	0.71±0.01	N/A	N/A
IVSd (mm)	0.67±0.01	0.67±0.01	0.70±0.01*	0.71±0.01*	N/A	N/A
LVIDd (mm)	4.15±0.07	4.08±0.08	3.65±0.14**	3.52±0.07**	N/A	N/A
LVIDs (mm)	3.37±0.07	3.24±0.10	3.20±0.15	3.15±0.06	N/A	N/A
FS (%)	18.76±0.69	20.55±1.11	12.34±1.24***	10.50±0.71***	N/A	N/A
SPWMD	3.26±0.65	4.08±0.58	26.55±5.0**	32.21±3.27***	N/A	N/A
LV Volumes						
EDV (µl)	78.78±3.83	82.93±4.27	57.95±6.07**	56.36±1.64***	N/A	N/A
ESV (µl)	45.11±1.98	48.09±2.40	42.25±4.5	46.05±1.66	N/A	N/A
EF (%)	42.58±1.04	41.86±1.31	26.77±2.27**	18.36±1.21***##	N/A	N/A
Tissue Doppler						
Maximal velocity (mm/s)	17.48±1.01	18.85±1.18	11.43±0.97**	9.37±0.40**	N/A	N/A
Minimal velocity (mm/s)	15.60±1.02	19.91±2.45	10.90±1.50**	7.28±0.64**#	N/A	N/A

Post-mortem biometric and mRNA data of wild-type (WT) and syndecan-4 knock-out (syn-4KO) mice 9 h after (post-) lipopolysaccharide (LPS)(10 mg/kg) injection and respective phosphate-buffered saline (PBS)-treated controls, n=12-13. Serial electrocardiographic and echocardiographic measurements of anesthetized WT and syn-4KO mice before (pre-) and 9 h after LPS (10 mg/kg) injection, n=8. BW, body weight; LVW, left ventricular weight; LW, lung weight; BNP, brain natriuretic peptide; Rpl4, ribosomal protein L4; AU, arbitrary units; QTc, QT corrected; LAD, left atrial diameter; LVPWd, left ventricular posterior wall thickness in diastole; IVSd, interventricular septum thickness in diastole; LVIDd, left ventricular internal diameter in diastole; LVIDs, left ventricular internal diameter in systole; FS, fractional shortening; EDV, end-diastolic volume; ESV, end-systolic volume; EF, ejection fraction; SPWMD, septal-to-posterior wall motion delay. Data are presented as mean ± S.E.M. Statistical differences were tested using Student's paired *t*-test (post-LPS vs. pre-LPS) or unpaired *t*-test (post-LPS vs. post-PBS); **P*<0.05; ***P*<0.01; ****P*<0.001, in respective genotype groups, or an unpaired *t*-test; $^{\#}P$<0.05; $^{\#\#}P$<0.01, syn-4KO post-LPS vs. WT post-LPS.

Figure legends

Fig.1 Increased cardiac syndecan-4 expression and shedding after LPS challenge *in vivo* and *in vitro*
Relative mRNA expression of syndecan-4 in left ventricles (LVs) of wild-type (WT) mice 9 h after lipopolysaccharide (LPS)(10 mg/kg) injection, compared to phosphate-buffered saline (PBS) controls, n=7-8 (A). Representative immunoblots and quantitative data of full-length (FL; upper) syndecan-4 and the ~10-15 kDa cellular fragment (CF; lower) remaining after shedding of syndecan-4 in LV lysates after methanol (MetOH) precipitation and treatment with heparan sulfate (HS)-degrading enzymes, n=3 (B). Schematic illustrating the antibody recognizing the CF of syndecan-4 (C). Plasma concentrations of syndecan-4 (ng/ml) 9 h after LPS injection, compared to PBS-injected controls, n=9 (D). Relative mRNA levels of syndecan-4 in neonatal rat cardiomyocytes (E) and cardiac fibroblasts (F) following 24 h treatment with LPS compared to co-treatment with the NF-κB inhibitor SM7368, n=8-10. Representative immunoblots and quantitative data of FL (upper) syndecan-4 and CF (lower), in LPS-stimulated cardiomyocytes (G) and cardiac fibroblasts (H) treated with MetOH and HS-degrading enzymes, n=3. Representative immunoblots of syndecan-4 CF in cardiomyocytes (I) and cardiac fibroblasts (J) following 24 h treatment with LPS compared to co-treatment with SM7368, n=6. mRNA data were normalized to ribosomal protein L4 (Rpl4) and actin was used for protein loading control. The lower panels in B, G and F are segments of the same blots as the upper panels, with longer exposure to visualize the CF of syndecan-4. The data are presented as mean ± S.E.M. Statistical differences were tested using Mann-Whitney test (B, G and H), Student's unpaired *t*-test (A, D), or one-way ANOVA with Bonferroni post-hoc test (E, F). **P*<0.05; ***P*<0.01; ****P*<0.001, significantly different from PBS or non-treated control; $^{\#\#\#}P$<0.001, significantly different from LPS treatment.

Fig.2 Expression of shedding enzymes is increased after LPS challenge
Relative mRNA levels of shedding enzymes a disintegrin and metalloproteinase (ADAM) with thrombospondin motifs (ADAMTS)1 (A) and 4 (B), matrix metalloproteinase (MMP)9 (C) and 2 (D) and ADAM17 (E) in the left ventricles (LVs) of wild-type (WT) mice 9 h after lipopolysaccharide (LPS)(10 mg/kg) injection, compared to phosphate-buffered saline (PBS) controls, n=7-8. mRNA data were normalized to ribosomal protein L4 (Rpl4) and presented as mean ± S.E.M. Statistical differences were tested using Student's unpaired *t*-test. **P*<0.05; ****P*<0.001, significantly different from PBS control.

Fig.3 LPS challenge leads to exacerbated cardiac dysfunction in syndecan-4 KO mice
End diastolic volume (A) in wild-type (WT) and syndecan-4 knock-out (syn-4KO) mice before (pre-LPS) and 9 h after (post-LPS) lipopolysaccharide (LPS)(10 mg/kg) injection, n=7-8. Representative tracings of the left ventricle in end-systole and end-diastole in long-axis echocardiography images, demonstrating reduced contraction post-LPS (B). Ejection fraction (EF; C) and diastolic tissue velocities (D) before and after LPS challenge. Representative tracings of electrocardiograms, demonstrating prolonged QRS duration and QT interval after LPS (E). See table I for animal characteristics. Statistical differences were tested using Student's paired t-test (post-LPS vs. pre-LPS) or unpaired t-test (WT vs. syn-4KO). ***P*<0.01; ****P*<0.001, significantly different from pre-LPS; $^{\#}P$<0.05; $^{\#\#}P$<0.01, syn-4KO significantly different from WT.

Fig.4 Reduced recruitment of immune cells to syndecan-4 KO hearts after LPS challenge *in vivo*
Relative mRNA levels of the T-cell marker genes CD8 (A), CD3 (B) and CD4 (C), the pan leukocyte marker CD11a (D), the macrophage marker F4/80 (E), tumor necrosis factor (TNF)α (F) and interleukin (IL)-1β (G) in left ventricles (LVs) of wild-type (WT) and syndecan-4 knock-out (syn-4KO) mice 9 h after lipopolysaccharide (LPS)(10 mg/kg) injection, relative to respective phosphate-buffered saline (PBS) controls, n=7-8. Data were normalized to ribosomal protein L4 (Rpl4) and presented as mean ± S.E.M. Statistical differences were tested using Student's unpaired *t*-test. **P*<0.05; ****P*<0.001, syn-4KO significant different from WT.

Fig.5 Shed syndecan-4 ectodomains induce innate immune signaling and receptors for immune cell recruitment in cardiac cells *in vitro*
Representative immunoblots showing levels of full-length (FL), the cellular fragment (CF) remaining in the cell after shedding of the ectodomain, and the shed ectodomain (SE) of syndecan-4 in cell lysates (A) and conditioned medium (B) from human endothelial kidney (HEK) 293 cells overexpressing full-length human influenza hemagglutinin (HA)-tagged syndecan-4 (HA-syn-4), n=6. Relative syndecan-4 levels (ng/ml) in conditioned medium analyzed by ELISA, n=6 (C). Relative mRNA levels of intercellular adhesion molecule (Icam)1 (D, F) and vascular cell adhesion molecule (Vcam)1 (E, G), tumor necrosis factor (TNF)α (H, J) and interleukin (IL)-1β (I, K) in cardiomyocytes and cardiac fibroblasts, respectively, after 24 h incubation with conditioned medium from HEK293 cells overexpressing syndecan-4 or syndecan-4 without heparan sulfate chains (syn-4 ΔHS), n=8-9. Controls consisted of non-treated cells and cells incubated with conditioned medium from HEK293 cells transfected with an empty vector (vehicle). Representative immunoblots and quantitative data of the p65 subunit of NF-κB (upper) and the NF-κB inhibitor protein IκBα (middle) after 24 h incubation with conditioned medium in cardiomyocytes (L) and cardiac fibroblasts (M), n=6. Relative mRNA levels of Icam1 (N) and Vcam1 (O) in left ventricles (LVs) of wild-type (WT) and syndecan-4 knock-out (syn-4KO) mice 9 h after lipopolysaccharide (LPS)(10 mg/kg) injection, relative to respective phosphate-buffered saline (PBS) controls, n=7-8. Data were normalized to ribosomal protein L4 (Rpl4) and presented as mean ± S.E.M. Actin was used for loading control. Statistical differences were tested using Student's unpaired *t*-test (C, N and O) or one-way ANOVA with Bonferroni post-hoc test (D-M). **P*<0.05; ***P*<0.01; ****P*<0.001, significantly different from non-transfected, non-treated or PBS control or syn-4KO significantly different from WT; $^{\#}P$<0.05; $^{\#\#}P$<0.01; $^{\#\#\#}P$<0.001, significantly different from vehicle or syn-4 ΔHS.

Fig.6 Shed syndecan-4 ectodomains regulate ECM remodeling in cardiac fibroblasts *in vitro*
Relative mRNA levels of smooth muscle α-actin (α-SMA; A), collagen I (B) and III (C) and proliferating cell nuclear antigen (PCNA; D) in cardiac fibroblasts following 24 h treatment with lipopolysaccharide (LPS), n=12. Relative mRNA levels of α-SMA (E), collagen I (F) and III (G) and total collagen (H) in left ventricles (LVs) of wild-type (WT) mice 9 h after LPS (10 mg/kg) injection, compared to phosphate-buffered saline (PBS)-injected controls, n=7-8. Relative mRNA of lysyl oxidase (LOX) in cardiac fibroblasts following 24 h treatment with LPS (I) and LVs of WT mice 9 h after LPS injection, compared to PBS controls (J). Relative mRNA of LOX (K) and collagen I (L) and III (M), matrix metalloproteinase (MMP)2 (N), 7 (O) and 9 (P), membrane type 1-MMP (Q), tissue inhibitor of metalloproteinase (TIMP) 1 (R), 2 (S), 3 (T) and 4 (U), in cardiac fibroblasts after 24 h incubation with conditioned medium from HEK293 cells overexpressing syndecan-4 or

syndecan-4 without heparan sulfate chains (syn-4 ΔHS), n=8-9. Relative mRNA levels of alpha skeletal muscle actin (Acta1; V) and PCNA (W) after 24 h incubation with conditioned medium in cardiomyocytes and cardiac fibroblasts, respectively, n=8-9. Controls consisted of non-treated cells and cells incubated with conditioned medium from HEK293 cells transfected with an empty vector (vehicle). Data were normalized to ribosomal protein L4 (Rpl4) and presented as mean ± S.E.M. Statistical differences were tested using Student's unpaired *t*-test (A-I) or one-way ANOVA with Bonferroni post-hoc test (J). **P*<0.05; ***P*<0.01; ****P*<0.001, significantly different from non-treated or PBS control; $^{\#}P$<0.5; $^{\#\#}P$<0.01; $^{\#\#\#}P$<0.001, significantly different from vehicle or syn-4 ΔHS.

Fig.7 Syndecan-4 is shed from the human heart
Relative syndecan-4 levels (ng/ml) in venous (V) blood from the coronary sinus of aortic stenosis patients obtained during open heart surgery, compared to arterial (A) blood from the radial artery of the same patient (n=30). Statistical differences were tested using Student's paired *t*-test. ***P*<0.01.

Figure 1

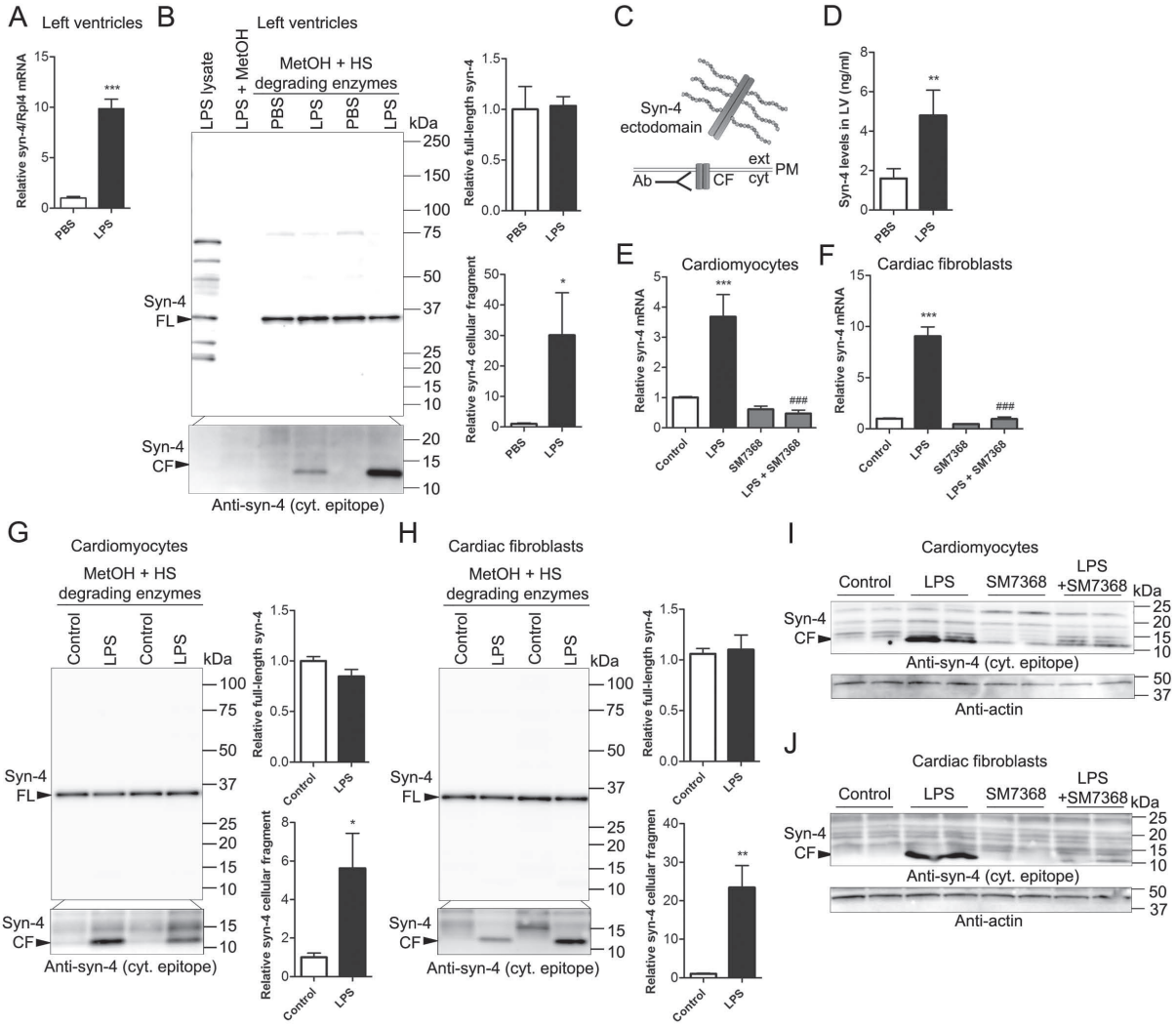
A
Left ventricles
Relative syn-4/Rpl4 mRNA
PBS
LPS
B
Left ventricles
LPS lysate
LPS + MetOH
MetOH + HS degrading enzymes
PBS
LPS
PBS
LPS
kDa
Syn-4 FL
Syn-4 CF
Anti-syn-4 (cyt. epitope)
Relative full-length syn-4
Relative syn-4 cellular fragment
C
Syn-4 ectodomain
ext
cyt
PM
Ab
CF
D
Syn-4 levels in LV (ng/ml)
E
Cardiomyocytes
Relative syn-4 mRNA
Control
LPS
SM7368
LPS + SM7368
F
Cardiac fibroblasts
G
Cardiomyocytes
MetOH + HS degrading enzymes
H
Cardiac fibroblasts
I
Cardiomyocytes
Control
LPS
SM7368
LPS +SM7368
Anti-actin
J
Cardiac fibroblasts

Figure 2

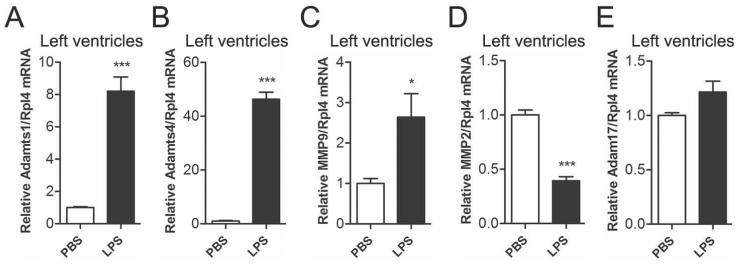
A
Left ventricles
Relative Adamts1/Rpl4 mRNA
10
8
6
4
2
0
***
PBS
LPS
B
Left ventricles
Relative Adamts4/Rpl4 mRNA
60
40
20
0
***
PBS
LPS
C
Left ventricles
Relative MMP9/Rpl4 mRNA
4
3
2
1
0
*
PBS
LPS
D
Left ventricles
Relative MMP2/Rpl4 mRNA
1.5
1.0
0.5
0.0
***
PBS
LPS
E
Left ventricles
Relative Adam17/Rpl4 mRNA
1.5
1.0
0.5
0.0
PBS
LPS

Figure 3

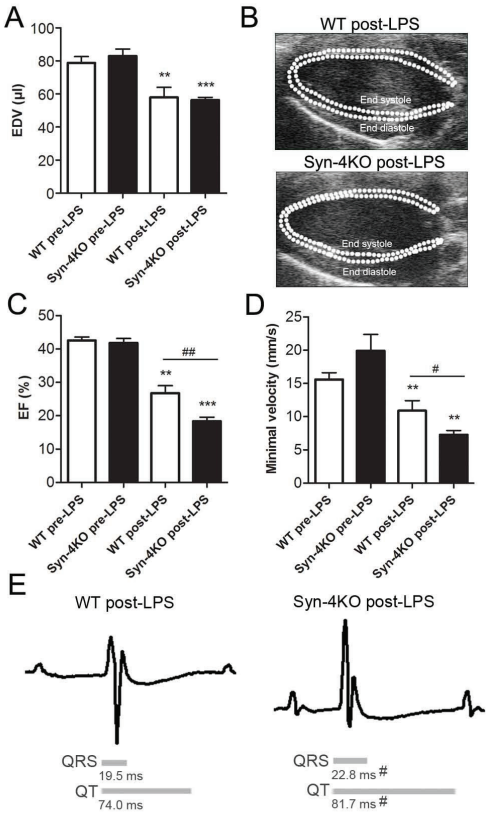
A
EDV (µl)
100
80
60
40
20
0
**
***
WT pre-LPS
Syn-4KO pre-LPS
WT post-LPS
Syn-4KO post-LPS
B
WT post-LPS
End systole
End diastole
Syn-4KO post-LPS
End systole
End diastole
C
EF (%)
50
40
30
20
10
0
##
**
***
WT pre-LPS
Syn-4KO pre-LPS
WT post-LPS
Syn-4KO post-LPS
D
Minimal velocity (mm/s)
25
20
15
10
5
0
#
**
**
WT pre-LPS
Syn-4KO pre-LPS
WT post-LPS
Syn-4KO post-LPS
E
WT post-LPS
Syn-4KO post-LPS
QRS
19.5 ms
QT
74.0 ms
QRS
22.8 ms #
QT
81.7 ms #

Figure 4

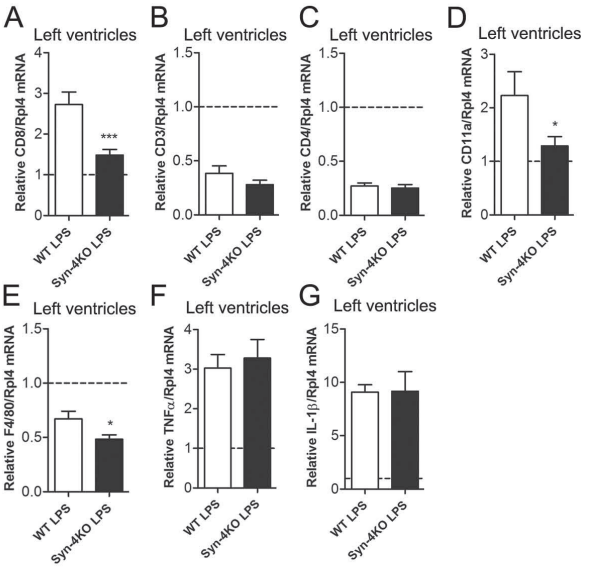
A
Left ventricles
Relative CD8/Rpl4 mRNA
***
WT LPS
Syn-4KO LPS
B
Left ventricles
Relative CD3/Rpl4 mRNA
C
Left ventricles
Relative CD4/Rpl4 mRNA
D
Left ventricles
Relative CD11a/Rpl4 mRNA
*
E
Left ventricles
Relative F4/80/Rpl4 mRNA
*
F
Left ventricles
Relative TNFα/Rpl4 mRNA
G
Left ventricles
Relative IL-1β/Rpl4 mRNA

Figure 5

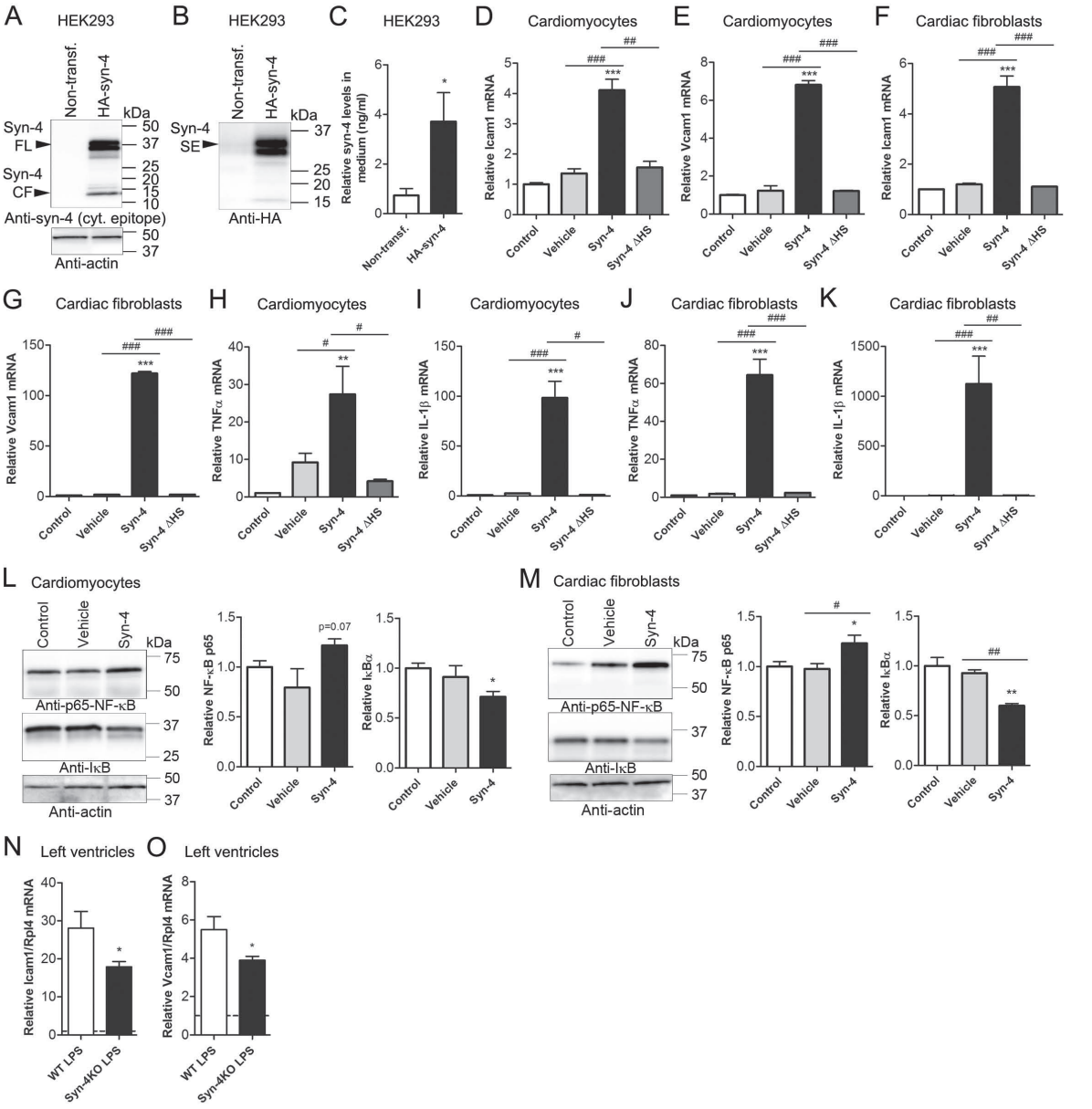
A
HEK293
Non-transf.
HA-syn-4
kDa
Syn-4 FL
Syn-4 CF
50
37
25
20
15
10
Anti-syn-4 (cyt. epitope)
Anti-actin
B
HEK293
Syn-4 SE
Anti-HA
C
HEK293
Relative syn-4 levels in medium (ng/ml)
D
Cardiomyocytes
Relative Icam1 mRNA
E
Cardiomyocytes
Relative Vcam1 mRNA
F
Cardiac fibroblasts
Relative Icam1 mRNA
Control
Vehicle
Syn-4
Syn-4 ΔHS
G
Cardiac fibroblasts
Relative Vcam1 mRNA
H
Cardiomyocytes
Relative TNFα mRNA
I
Cardiomyocytes
Relative IL-1β mRNA
J
Cardiac fibroblasts
Relative TNFα mRNA
K
Cardiac fibroblasts
Relative IL-1β mRNA
L
Cardiomyocytes
Anti-p65-NF-κB
Anti-IκB
Anti-actin
Relative NF-κB p65
p=0.07
Relative IκBα
M
Cardiac fibroblasts
N
Left ventricles
Relative Icam1/Rpl4 mRNA
WT LPS
Syn-4KO LPS
O
Left ventricles
Relative Vcam1/Rpl4 mRNA

Figure 6

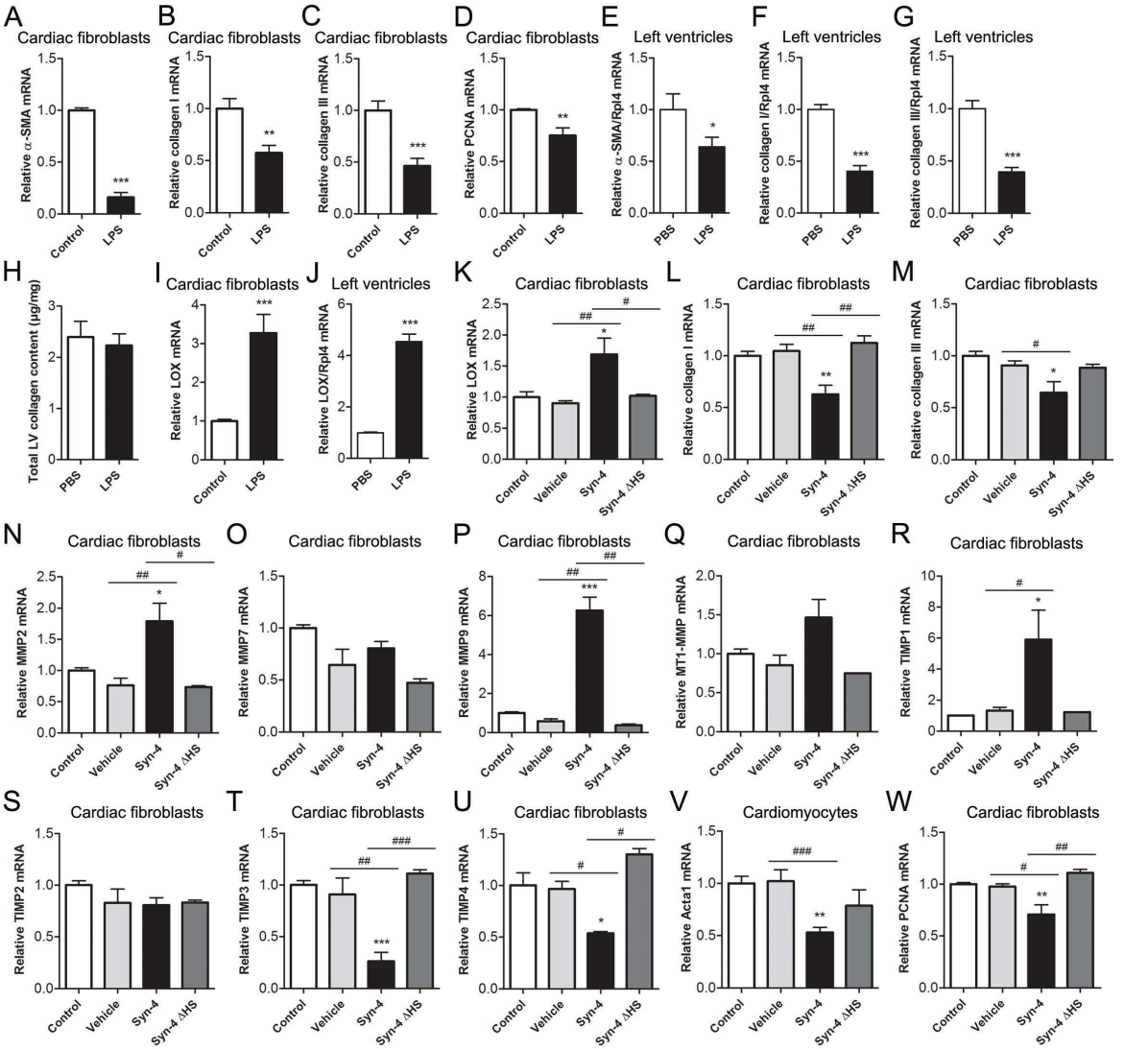
A
Cardiac fibroblasts
Relative α-SMA mRNA
Control
LPS
B
Cardiac fibroblasts
Relative collagen I mRNA
C
Cardiac fibroblasts
Relative collagen III mRNA
D
Cardiac fibroblasts
Relative PCNA mRNA
E
Left ventricles
Relative α-SMA/Rpl4 mRNA
PBS
F
Left ventricles
Relative collagen I/Rpl4 mRNA
G
Left ventricles
Relative collagen III/Rpl4 mRNA
H
Total LV collagen content (μg/mg)
I
Cardiac fibroblasts
Relative LOX mRNA
J
Left ventricles
Relative LOX/Rpl4 mRNA
K
Cardiac fibroblasts
Relative LOX mRNA
Vehicle
Syn-4
Syn-4 ΔHS
L
Cardiac fibroblasts
Relative collagen I mRNA
M
Cardiac fibroblasts
Relative collagen III mRNA
N
Cardiac fibroblasts
Relative MMP2 mRNA
O
Cardiac fibroblasts
Relative MMP7 mRNA
P
Cardiac fibroblasts
Relative MMP9 mRNA
Q
Cardiac fibroblasts
Relative MT1-MMP mRNA
R
Cardiac fibroblasts
Relative TIMP1 mRNA
S
Cardiac fibroblasts
Relative TIMP2 mRNA
T
Cardiac fibroblasts
Relative TIMP3 mRNA
U
Cardiac fibroblasts
Relative TIMP4 mRNA
V
Cardiomyocytes
Relative Acta1 mRNA
W
Cardiac fibroblasts
Relative PCNA mRNA

Figure 7

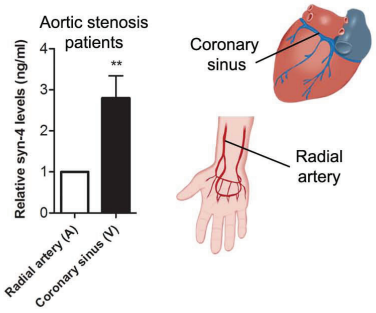
Aortic stenosis patients
Relative syn-4 levels (ng/ml)
4
3
2
1
0
**
Radial artery (A)
Coronary sinus (V)
Coronary sinus
Radial artery

Supplemental Material

Detailed Methods

Human blood samples

Thirty consecutive patients operated for severe, symptomatic aortic stenosis (AS) with aortic valve replacement (AVR) at Oslo University Hospital Ullevål, Oslo, Norway, were included in this study and were part of a previously published cohort [1]. Blood samples (10 ml each) were drawn during open heart surgery from a coronary sinus catheter and from the cannulated radial artery immediately after onset of cardiopulmonary bypass. Chilled EDTA tubes (1mg/ml blood) were used and kept on ice before centrifugation within 30 min. Serum and plasma fractions were separated and stored at -70°C until analyzed. Serum syndecan-4 levels were analyzed using a human syndecan-4 ELISA kit (27188, IBL, Gunma, Japan) according to protocol. This assay has a detection limit of 20 pg/ml.

Mouse model of LPS challenge

Eight-ten week old male wild-type (WT) C57BL/6JBomTac (Taconic, Skensved, Denmark) and syndecan-4 knock-out (KO) mice [2] were randomized to intraperitoneal injection with a single dose of LPS (10 mg/kg, *Escherichia coli* O111:B4, List Biological Laboratories Inc., Campbell, CA) dissolved in sterile phosphate-buffered saline (PBS) or an equivalent volume of PBS (control). Echocardiographic examinations were performed on anesthetized mice breathing a mixture of 1.75% isoflurane and 98.25% O_2 on a mask using VEVO 2100 (VisualSonics, Toronto, Canada) before (pre-LPS) and 9 h after (post-LPS) injections, n=8. Long and short axis images of left ventricle (LV) and left atrium were obtained, in addition to tissue Doppler in the LV posterior wall. Electrocardiography (ECG), heart rate and respiration were obtained with the VEVO 2100 physiology monitoring system. Echocardiographic and ECG data were analyzed offline using VEVO 2100 1.1.0 software from VisualSonics by an experienced investigator blinded to genotype and treatment. End diastolic and end systolic volumes (EDV and ESV, respectively) were calculated by the Vevo 2100 software by tracing the left ventricular border in end systole and diastole. Three representative cycles were analyzed and averaged. ECG analyses were performed by first defining the isoelectric line as the signal from the end of the T-wave to the P-wave of the subsequent heartbeat. The QRS-complex was defined as the first deviation from the isoelectric line after the P-wave to the last intersection of the isoelectric line before the T-wave. The QT time was defined as the start of the QRS complex to the T-wave returning to the isoelectric line. Five consecutive ECG signals were averaged. QTc time was calculated by the formula $QTc=QT/\sqrt{RR\text{-interval}}$ [3]. Mice were sacrificed by cervical dislocation 9 h after injections. Hearts, lungs and kidneys were rapidly excised, LVs dissected, snap-

frozen in liquid nitrogen and stored at -70°C, n=12-13. Body, LV and lung weights were measured, and LV and lung weights normalized to body weight. Organ weights and molecular biology analyses of tissues were compared among LPS-injected and PBS-injected control mice. In a separate cohort, blood was drawn from the left ventricle of anesthetized WT mice 9 h after LPS or PBS injection, n=9. Plasma was collected in chilled EDTA tubes (1 mg/ml) before centrifugation at 3000 g at 4 °C for 20 min and stored at -70 °C. Syndecan-4 levels were analyzed using a mouse syndecan-4 ELISA kit (E03S0065, Blue Gene, Shanghai, China), according to protocol. This assay has a detection limit of 250 pg/ml. Non-invasive blood pressure measurements were obtained from a separate cohort under light anesthesia before and after LPS with a tail-cuff-based CODA system (Kent Scientific, Torrington, CT) by an experienced researcher blinded to genotype, n=5-10. Each animal was subjected to serial measurements and blood pressures calculated as the mean of the recordings accepted by the CODA software. Blood was drawn from the abdominal aorta and blood urea nitrogen (BUN) was analyzed by a DetectX BUN kit (K024, Arbor Assays, Ann Arbor, MI), according to protocol.

HEK293 cell culture and transfection

HEK293 cells were cultured and transfected using Lipofectamine 2000 (Invitrogen, Paisley, UK) with an N-terminal human influenza hemagglutinin (HA)-tagged full-length syndecan-4 (NP_035651) in a pcDNA3.1 vector (Invitrogen; custom made by Genscript Corporation, Piscataway, NJ) and the same construct with S44/S62/S64 mutated to A44/A62/A64, essentially as described [4]. Non-transfection or transfection with an empty pcDNA3.1 vector (vehicle) served as controls. Protein lysate and conditioned medium were harvested after 24 h. The total volume medium (2 ml) was collected and cleared by centrifugation at 5000 g (conditioned medium). For immunoblot analyses, conditioned medium was concentrated using Amicon Ultra-4 centrifugal filters (3 kDa cut-off, Merck Millipore, Darmstadt, Germany). Conditioned medium syndecan-4 levels were analyzed using a syndecan-4 ELISA kit (27188, IBL).

Primary cultures of neonatal cardiac myocytes and fibroblasts

Primary rat cardiomyocyte and fibroblast cultures were prepared from 1-3 day old Wistar rats (Taconic) as described [5]. Briefly, LVs were dissected, digested mechanically and with collagenase, and transferred to uncoated culture flasks, allowing fibroblasts to attach. Unattached cells, i.e. cardiomyocytes, were transferred to gelatin and fibronectin-coated 6-well culture plates at a density of 3.75×10^5/ml medium. Fibroblasts were maintained in culture for up to one week, passaged and seeded onto 6-well culture plates at a density of 1.8×10^5/ml. Cells were kept in a 37°C, 5% CO_2 humidified incubator. Following 24 h of

serum deprivation, cells were stimulated for 9 or 24 h with LPS (1 µg/ml, 201, List Biological Laboratories), SM7368 (10 mM, 481411, Merck Millipore), CLI-095 (1 µg/ml, tlrl-cli95, InvivoGen, San Diego, CA) or 2 ml conditioned medium (diluted 2:1 in fresh medium) from HEK293 cells, harvested and stored at -70°C. Due to variation in responsiveness of primary cardiac cultures [6], cells from three separate isolations were used for all analyses.

RNA isolation and quantitative real-time PCR (qRT-PCR)

Total RNA was isolated from LVs and kidneys of mice and neonatal rat cells using RNeasy mini (74106, Qiagen Nordic, Oslo, Norway). RNA concentrations were measured using Nanodrop ND-1000 Spectrophotometer (Thermo Fisher Scientific, Waltham, MA). Samples with RNA integrity number (RIN) >7 determined on the 2100 Bioanalyzer (Agilent Technologies, Santa Clara, CA) were accepted. Reverse transcription was performed with the iScript cDNA Synthesis Kit (Bio-Rad Laboratories, Inc., Hercules, CA). The following pre-designed TaqMan assays (Applied Biosystems Foster City, CA) were used: mouse syndecan-4 (Mm00488527_m1), mouse ADAMTS1 (Mm004477355_m1), mouse ADAMTS4 (Mm00556068_m1), mouse MMP9 (Mm00442991_m1), mouse MMP2 (Mm00439506_m1), mouse ADAM17 (Mm00456428_m1), mouse KIM-1 (Mm00506686_m1), mouse NGAL (Mm01324470_m1), mouse CD8 (Mm01182107_g1), mouse CD3 (Mm01179194_m1), mouse CD4 (Mm00442754_m1), mouse IL-1β (Mm_01336189_m1), mouse TNFα (Mm00443258_m1), mouse CD45R (Mm01293575_m1), mouse CD11a (Mm00801807_m1), mouse F4/80 (Mm00802529_m1), (Mm01546133_m1), mouse Icam1 (Mm00516023_m1), mouse Vcam1 (Mm01320970_m1), mouse BNP (Mm00435304_g1), mouse α-SMA (Mm01546133_m1), mouse collagen I (Mm00483888_m1), mouse collagen III (Mm01254476_m1), mouse LOX (Mm00495386_m1), rat syndecan-4 (Rn00561900_m1), rat ADAMTS1 (Rn01646120_g1), rat ADAMTS4 (Rn02103282_s1), rat MMP9 (Rn00579162_m1), rat MMP2 (Rn01538177_m1), rat ADAM17 (Rn00571880_m1), rat Icam1 (Rn00564227_m1), rat Vcam1 (Rn00563627_m1), rat IL-1β (Rn00580432_m1), rat TNFα (Rn99999017_m1), rat α-SMA (Rn01759928_g1), rat collagen I (Rn01463848_m1), rat collagen III (Rn01437681_m1), rat PCNA (Rn01514538_g1), rat LOX (Rn01491829_m1), rat MMP7 (Rn00689241_m1), rat MT1-MMP (Rn00579172_m1), rat TIMP1 (Rn01430873_g1), rat TIMP2 (Rn00573232_m1), rat TIMP3 (Rn00441826_m1), rat TIMP4 (Rn01459160_m1), rat biglycan (Rn00567229_m1), rat decorin (Rn01503161_m1), rat fibromodulin (Rn00589918_m1), rat lumican (Rn00579127_m1), rat HAS1 (Rn01455687_g1), rat HAS2 (Rn00565774_m1) and rat Acta1 (Rn01426628_g1). Quantitative real-time PCR results were detected on an ABI PRISM 7900HT Sequence Detection System and analyzed using the Sequence Detection System 2.3 software (Applied Biosystems).

Protein isolation and immunoblotting

Snap-frozen LVs were homogenized using a Polytron 1200 in a PBS lysis buffer containing 1% Triton X-100 (Sigma, MI), 0.1% Tween-20 (Sigma) and protease inhibitors (Complete EDTA-free tablets, Roche Diagnostics, Oslo, Norway), incubated on ice for 30 min and centrifuged at 20 000 g for 10 min. Supernatants were stored at -70°C. Whole-cell lysates from HEK293 and neonatal rat cardiac cells were collected using the same lysis buffer as above. Samples were vortexed and the supernatant collected after centrifugation and stored at -70°C. A common challenge with immunoblotting of proteoglycans is the high number of bands that appear due to glycosylation and proteolytic cleavage. Enzymatic removal of GAG chains prior to gel electrophoresis enables the core protein to migrate as discrete bands of specific and expected molecular weights. For analyses of syndecan-4 protein levels, equal amounts (100 μg) of protein were precipitated using methanol before samples were treated with heparan sulfate-degrading enzymes (Heparitinase I, Heparitinase II, Heparitinase III and Chondritinase cABC (all from AMSBIO, Abingdon, UK)) as described [5]. SDS-PAGE and immunoblotting were performed according to the Criterion BIO-RAD protocol essentially as described [4]. Blots were blocked in non-fat dry milk (BIO-RAD) or casein (Roche Diagnostics), incubated with primary antibodies overnight and subsequently, species-appropriate secondary antibodies diluted in blocking solution. Blots were developed using ECL Prime (Amersham/GE HealthCare, Buckinghamshire, UK) in the Las-4000 (Fujifilm, Tokyo, Japan) and reprobed after stripping using the Western blot stripping buffer (210591, Thermo Scientific). Processing and quantification were performed using Adobe Photoshop CS5 and Image J (NIH), and the data normalized to loading controls. Primary antibodies used were: anti-syndecan-4 cytoplasmic epitope (custom made, Genscript Corporation), anti-IκBα (sc-371), anti-actin (sc-8432) and anti-glyceraldehyde 3-phosphate dehydrogenase (sc-20357, Santa Cruz Biotechnology, Santa Cruz, CA), anti-p65 NF-κB (8242) and anti-HA (3724, Cell Signaling Technology, Danvers, MA). HRP-conjugated secondary antibodies from Southern Biotechnology (Birmingham, AL) were applied to all blots. To assess shedding by immunoblotting, the transmembrane and cytoplasmic part of syndecan-4 remaining in the cells after shedding of the extracellular domain was detected using an antibody detecting a cytoplasmic epitope [4] of syndecan-4 (see Strand *et al*. [5] for details). In brief, several transfection experiments in cells using a number of syndecan-4 plasmid constructs and antibodies were performed to validate the specificity of this fragment. Thus, the 10-15 kDa band represents a membrane-localized, syndecan-4-specific fragment consisting of its transmembrane and cytoplasmic domains, remaining in cells after shedding of the ectodomain.

References

[1] Braathen B, Tønnessen T. Cold blood cardioplegia reduces the increase in cardiac enzyme levels compared with cold crystalloid cardioplegia in patients undergoing aortic valve replacement for isolated aortic stenosis. J Thorac Cardiovasc Surg. 2010;139:874-80.
[2] Echtermeyer F, Streit M, Wilcox-Adelman S, Saoncella S, Denhez F, Detmar M, et al. Delayed wound repair and impaired angiogenesis in mice lacking syndecan-4. J Clin Invest. 2001;107:R9-R14.
[3] Mitchell GF, Jeron A, Koren G. Measurement of heart rate and Q-T interval in the conscious mouse. Am J Physiol Heart Circ Physiol. 1998;274:H747-H51.
[4] Finsen AV, Lunde IG, Sjaastad I, Østli EK, Lyngra M, Jarstadmarken HO, et al. Syndecan-4 is essential for development of concentric myocardial hypertrophy via stretch-induced activation of the calcineurin-NFAT pathway. PLoS ONE. 2011;6:e28302.
[5] Strand ME, Herum KM, Rana ZA, Skrbic B, Askevold ET, Dahl CP, et al. Innate immune signaling induces expression and shedding of the heparan sulfate proteoglycan syndecan-4 in cardiac fibroblasts and myocytes, affecting inflammation in the pressure-overloaded heart. FEBS J. 2013;280:2228-47.
[6] Louch WE, Sheehan KA, Wolska BM. Methods in cardiomyocyte isolation, culture, and gene transfer. J Mol Cell Cardiol. 2011;51:288-98.
[7] Vaidya VS, Ferguson MA, Bonventre JV. Biomarkers of acute kidney injury. Annu Rev Pharmacol Toxicol. 2008;48:463-93.
[8] Supavekin S, Zhang W, Kucherlapati R, Kaskel FJ, Moore LC, Devarajan P. Differential gene expression following early renal ischemia/reperfusion. Kidney Int. 2003;63:1714-24.
[9] Ichimura T, Bonventre JV, Bailly V, Wei H, Hession CA, Cate RL, et al. Kidney injury molecule-1 (KIM-1), a putative epithelial cell adhesion molecule containing a novel immunoglobulin domain, is up-regulated in renal cells after injury. J Biol Chem. 1998;273:4135-42.

Supplemental Figures

Supplemental Figure S1

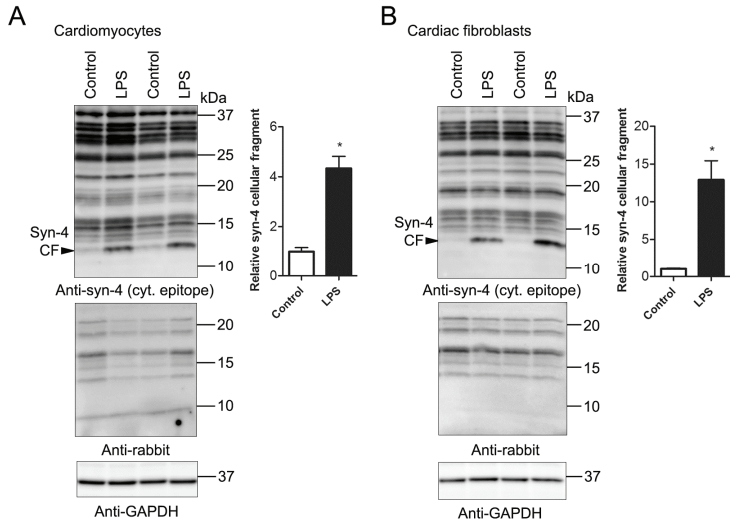

Fig. S1 LPS induces syndecan-4 shedding in cardiac cells *in vitro*. Representative immunoblots and quantitative data of the ~10-15 kDa cellular fragment (CF) remaining in cells after ectodomain shedding of syndecan-4 (upper) following 9 h of lipopolysaccharide (LPS) treatment in cardiomyocytes (A) and cardiac fibroblasts (B), n=3. See Strand *et al.* for details on this syndecan-4-specific band. Immunoblots probed only with secondary antibody (middle), showing unspecific bands. Glyceraldehyde 3-phosphate dehydrogenase (GAPDH; lower) was used for loading control. Statistical differences were tested using Mann-Whitney test. **P*<0.05, significantly different from non-treated control.

Supplemental Figure S2

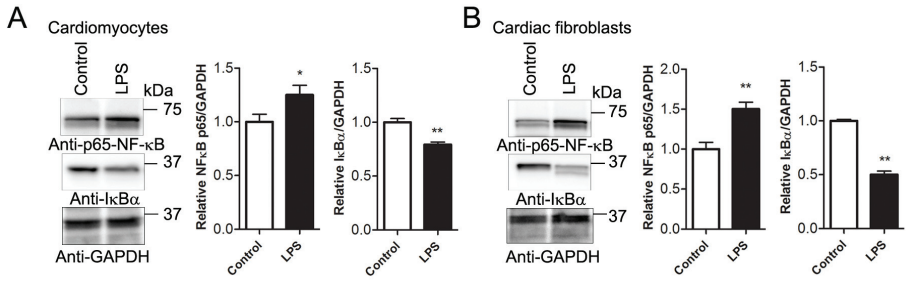

Fig. S2 LPS activates NF-κB signaling in cardiac cells *in vitro*. Representative immunoblots and quantitative data of the p65 subunit of nuclear factor (NF)-κB (upper) and the NF-κB inhibitor protein IκBα (middle) following 24 h of lipopolysaccharide (LPS) treatment in cardiomyocytes (A) and cardiac fibroblasts (B), n=6. Glyceraldehyde 3-phosphate dehydrogenase (GAPDH) was used for loading control. Statistical differences were tested using Student's unpaired *t*-test. **P*<0.05; ***P*<0.01, significantly different from non-treated control.

Supplemental Figure S3

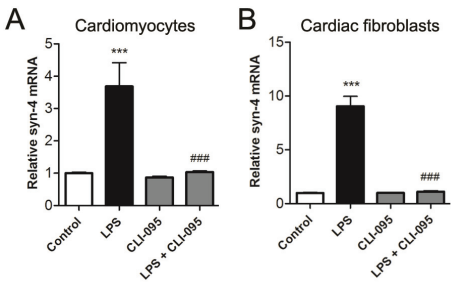

Fig. S3 LPS induces syndecan-4 mRNA through toll-like receptor 4. Relative mRNA levels of syndecan-4 in cardiomyocytes (A) and cardiac fibroblasts (B) following 24 h of lipopolysaccharide (LPS) treatment compared to co-treatment with the toll-like receptor 4 inhibitor CLI-095, n=7-9. Statistical differences were tested using one-way ANOVA with Bonferroni post-hoc test. ***P<0.001, significantly different from non-treated control; $^{###}P$<0.001, significantly different from LPS treatment.

Supplemental Figure S4

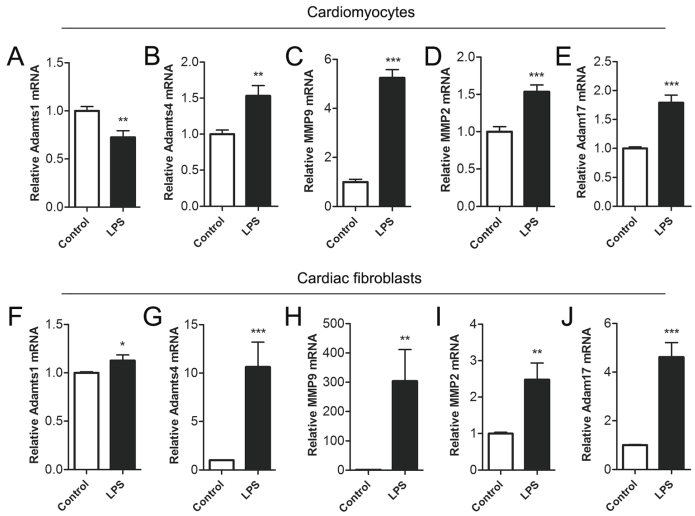

Fig. S4 LPS induces expression of shedding enzymes in cardiac cells *in vitro*. Relative mRNA levels of shedding enzymes a disintegrin and metalloproteinase (ADAM) with thrombospondin motifs (ADAMTS)1 (A, F) and 4 (B, G), matrix metalloproteinase (MMP)9 (C, H) and 2 (D, I) and ADAM17 (E, J) in cardiomyocytes and cardiac fibroblasts, respectively, following 24 h of lipopolysaccharide (LPS) treatment, n=6-12. Statistical differences were tested using Student's unpaired *t*-test. **P*<0.05; ***P*<0.01; ****P*<0.001, significantly different from non-treated control.

Supplemental Figure S5

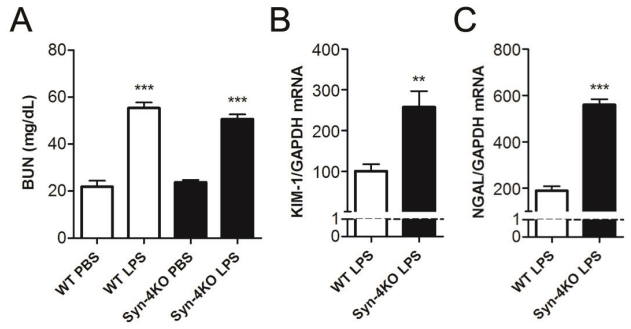

Fig. S5 LPS induces kidney dysfunction and injury in syndecan-4 KO and WT mice. Blood (plasma) concentrations of urea nitrogen (BUN; mg/dL) as indication of kidney dysfunction in wild-type (WT) and syndecan-4 knock-out (syn-4KO) mice 9 h after lipopolysaccharide (LPS)(10 mg/kg) or phosphate-buffered saline (PBS) injections (A), n=5-10. Relative mRNA levels of the kidney injury markers [7-9] kidney injury molecule (KIM)-1 (B) and neutrophil gelatinase associated lipocalin (NGAL) (C) in kidneys of WT and syn-4KO mice 9 h after LPS injection, compared to respective PBS-treated controls. mRNA data were normalized to glyceraldehyde 3-phosphate dehydrogenase (GAPDH). Statistical differences were tested using Student's unpaired *t*-test. ***P*<0.01; ****P*<0.001, significantly different from PBS control.

Supplemental Figure S6

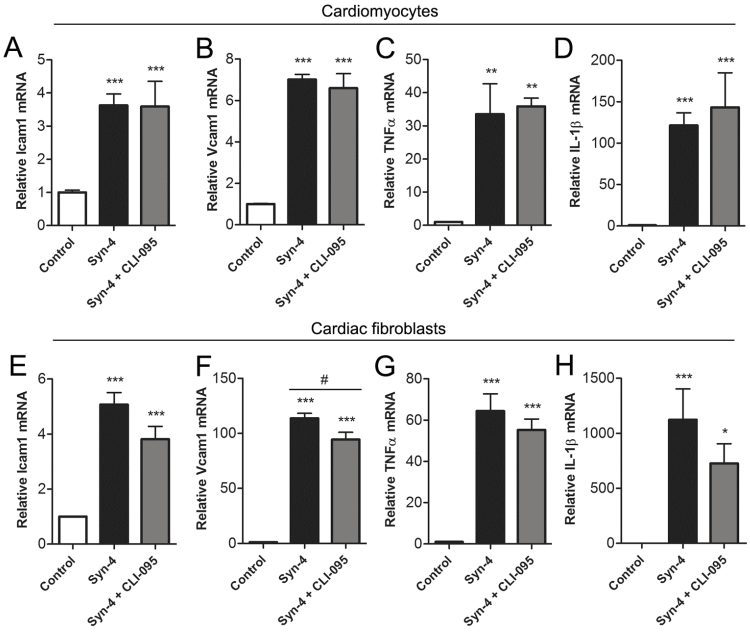

Fig. S6 Shed syndecan-4 does not signal through toll-like receptor 4 in cardiac cells. Relative mRNA levels of intercellular adhesion molecule (Icam)1 (A, E), vascular cell adhesion molecule (Vcam)1 (B, F), tumor necrosis factor (TNF)α (C, G) and interleukin (IL)-1β (D, H) in cardiomyocytes and cardiac fibroblasts, respectively, after 24 h of incubation with conditioned medium from HEK293 cells overexpressing syndecan-4, compared to co-treatment with the toll-like receptor 4 inhibitor CLI-095, n=7-9. Statistical differences were tested using one-way ANOVA with Bonferroni post-hoc test. **P*<0.05; ***P*<0.01; ****P*<0.001, significantly different from unstimulated controls. $^{\#}$*P*<0.05, significantly different from co-treatment with CLI-095.

Supplemental Figure S7

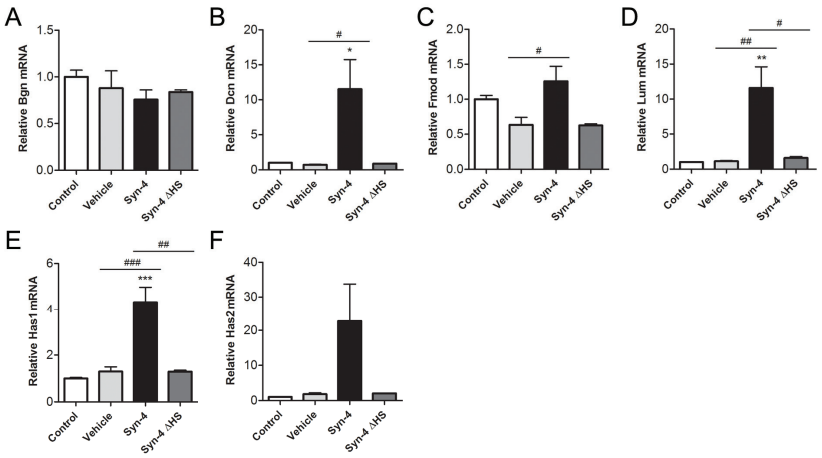

Fig. S7 Shed syndecan-4 regulates expression of ECM molecules in cardiac fibroblasts. Relative mRNA levels of biglycan (Bgn; A), decorin (Dcn; B), fibromodulin (Fmod; C), lumican (Lum; D), hyaluronan synthases (Has) 1 (E) and 2 (F) in cardiac fibroblasts, after 24 h of incubation with conditioned medium from HEK293 cells overexpressing syndecan-4 or syndecan-4 without heparan sulfate chains (syn-4 ΔHS), n=8-9. Statistical differences were tested using one-way ANOVA with Bonferroni post-hoc test.*P<0.05; **P<0.01; ***P<0.001, significantly different from unstimulated controls. $^{\#}P$<0.05; $^{\#\#}P$<0.01; $^{\#\#\#}P$<0.001 significantly different from vehicle or syn-4 ΔHS.

Supplemental Tables

Supplemental Table SI

Table SI Blood pressure of syndecan-4 KO and WT mice after LPS challenge

	Baseline		Post-LPS		Post-PBS	
	WT	**Syn-4KO**	**WT**	**Syn-4KO**	**WT**	**Syn-4KO**
N	15	15	10	10	5	5
Systolic BP (mmHg)	123.00±2.80	115.40±3.17	93.87±4.38**	102.90±5.33*	120.40±2.75	116.70±7.94
Diastolic BP (mmHg)	93.29±2.62	84.45±3.05	60.25±3.48***	70.48±5.80*	90.92±2.44	89.20±6.62

Tail-cuff blood pressure (BP) measurements of wild-type (WT) and syndecan-4 knock-out (syn-4KO) mice under light anesthesia, before (baseline) and 9 h after (post-) lipopolysaccharide (LPS)(10 mg/kg) or phosphate-buffered saline (PBS) injection, n=5-10. mmHg, millimeter of mercury. Data are presented as mean ± S.E.M. Statistical differences were tested using Student's unpaired *t*-test; **P*<0.05; ***P*<0.01; ****P*<0.001, post-LPS vs. baseline in respective genotype groups. Student's unpaired *t*-test revealed no difference in systolic or diastolic BP between the two genotypes post-LPS.

Supplemental Table SII

Table SII Clinical characteristics of aortic stenosis (AS) patients

	AS patients
N	30
Female sex, n	13
Age	70.4±1.7
CPB time, min	103.8±3.0
Cross-clamp time, min	73.4±3.1
Pre-operative ejection fraction, %	50.8±0.2
IVSd, cm	1.4±0.1
Postoperative atrial fibrillation, n	12
Myocardial infarction, n	0
30-day mortality, n	0
Preoperative use of β-blockers, n	7
Postoperative use of β-blockers, n	22
Aspirin	8
Statins	6
Nitrates	3
ACE-inhibitors	5
Calcium channel blockers	4

Thirty patients with severe aortic stenosis (AS) undergoing aortic valve replacement were prospectively included in this study. Patient characteristics and preoperative data are presented as mean ± S.E.M. CPB, cardiopulmonary bypass; IVSd, interventricular septal thickness at diastole; ACE, angiotensin-converting enzyme.